



Faculty of Engineering Science  
**Department of Mechanical Engineering**  
Celestijnenlaan 300 – box 2420 – B-3001 Heverlee

# Rotational casting machine

<b>Date</b>	22/05/2025
<b>Course</b>	H04P9A – H00S1A
<b>Type</b>	Final report
<b>Access</b>	Public
<b>Authors</b>	Thewis Jonas (0883471) Van Geyseghem Jarne (r0885062) Vanhees Rik (r0885864) Van Wayenberge Renaat (r0891107)
<b>Commissioned by</b>	KU Leuven
<b>Commissioning supervisors</b>	Roels Ellen Gorissen Benjamin
<b>Supervisors KU Leuven</b>	Roels Ellen Gorissen Benjamin

## Abstract

This report details the design, fabrication, and initial testing of a novel rotational casting machine developed for the manufacturing of hollow silicone components, specifically tailored for the fabrication of soft robotic actuators in a research environment. To address current limitations in traditional fabrication methods that often require multi-part molds, and subsequent assembly, this machine utilizes a bi-axial rotation system to achieve uniform material distribution around a mold interior. The design of the entire machine is presented, including the mechanical, electronic and software aspects. It integrates a Raspberry Pi Pico for control, managing stepper motors through advanced TMC2130 stepper drivers, a thermistor controlled PTC heating element to accelerate curing, and a user-friendly interface all with the necessary safety interlocks. The mechanical design features a rigid aluminum frame, safe enclosure, advanced belt transmission, and a versatile perforated plate mounting system. While the machine successfully demonstrates its core functionality and meets all functional requirements, preliminary tests reveal the need for further research into optimal silicone compositions, rotation speeds, and heating profiles to achieve uniform wall thicknesses. This project delivers a functional and cost-effective (totaling €611.73) platform, providing the tools further research in the fabrication of soft robotics and development of more advanced machines and processes.

# Contents

<b>1</b>	<b>Introduction</b>	<b>1</b>
<b>2</b>	<b>Requirements</b>	<b>2</b>
<b>3</b>	<b>Conceptual design</b>	<b>3</b>
3.1	Bi-axial rotation . . . . .	3
3.2	Generation of rotational motion . . . . .	5
3.3	Connecting the mold . . . . .	6
3.4	Heating . . . . .	7
<b>4</b>	<b>Mechanical design</b>	<b>9</b>
4.1	Frame . . . . .	9
4.2	Kinematics . . . . .	10
4.3	Motor selection . . . . .	13
4.4	Mounting system . . . . .	14
4.5	Enclosure . . . . .	17
4.6	Heater . . . . .	19
<b>5</b>	<b>Electrical design</b>	<b>23</b>
5.1	Stepper driver . . . . .	23
5.2	Heater . . . . .	24
5.3	Fans . . . . .	24
5.4	Power . . . . .	26
5.5	Microcontroller . . . . .	27
5.6	Fuse . . . . .	27
5.7	E-stop . . . . .	28
5.8	Limit switch . . . . .	28
5.9	Power socket . . . . .	29
5.10	Display . . . . .	29
5.11	Rotary push-button . . . . .	30
5.12	LED-strip . . . . .	30
5.13	Buzzer . . . . .	31
<b>6</b>	<b>Software</b>	<b>34</b>
6.1	Finite state machine . . . . .	34
6.2	Sensor information . . . . .	34
6.3	Flash . . . . .	35
6.4	User interface . . . . .	36
6.5	LED strip . . . . .	36
6.6	Stepper motor control . . . . .	36
6.7	Heater control . . . . .	37
<b>7</b>	<b>Budget</b>	<b>38</b>
<b>8</b>	<b>Testing</b>	<b>39</b>
8.1	Overview of test . . . . .	39
8.2	Machine performance . . . . .	40
<b>9</b>	<b>Conclusion</b>	<b>44</b>
<b>A</b>	<b>Machine documentation</b>	<b>46</b>
A.1	Quickstart guide . . . . .	46
A.2	Maintenance . . . . .	47

A.3	Flashing new software . . . . .	49
A.4	Documentation of software . . . . .	49
<b>B</b>	<b>Logbook</b>	<b>51</b>
<b>C</b>	<b>Gantt chart</b>	<b>54</b>

## List of Figures

1	Example of a bi-axial rotating frame construction used in an industrial machine [1] . . . . .	3
2	Example of transmission based rotational casting machine . . . . .	4
3	Proposed alternate clamping system . . . . .	6
4	Illustration of perforated plate . . . . .	7
5	Frame . . . . .	9
6	Blind joint technique used on the frame . . . . .	10
7	Rotation axis of the machine . . . . .	11
8	Belt transmissions . . . . .	12
9	Belt tensioner . . . . .	13
10	17HE24-2104S Torque graph . . . . .	14
11	Plate system overview . . . . .	14
12	Plate FEA results . . . . .	16
13	Slider overview . . . . .	16
14	Sliding bracket . . . . .	17
15	Enclosure . . . . .	18
16	Assembled Machine . . . . .	19
17	Simulated temperature inside the machine due to the PTC heater . . . . .	20
18	Heating unit position . . . . .	21
19	Heating unit versions . . . . .	22
20	Stepper Motor Driver Schematic in KiCad . . . . .	23
21	Enable Driver Schematic in KiCad . . . . .	24
22	Heater and fuse in KiCad . . . . .	24
23	Fan next to heater Schematic in KiCad . . . . .	25
24	Fans to cool PCB Schematic in KiCad . . . . .	25
25	Thermistor in KiCad . . . . .	26
26	24V Converter Schematic in KiCad . . . . .	26
27	5V Converter Schematic in KiCad . . . . .	26
28	Raspberry PI Pico Schematic in KiCad . . . . .	27
29	E-stop Schematic in KiCad . . . . .	28
30	Limit switch Schematic in KiCad . . . . .	29
31	Screen Schematic in KiCad . . . . .	30
32	Rotary push-button Schematic in KiCad . . . . .	30
33	LED Schematic in KiCad . . . . .	31
34	Buzzer Schematic in KiCad . . . . .	31
35	PCB integration on CAD model . . . . .	33
36	Electrical wiring . . . . .	33
37	Experimental mold and results . . . . .	40
38	Second test - silicone light bulb . . . . .	40
39	Enclosure heating test results . . . . .	41
40	PCB integration with jumper marking . . . . .	43
41	Extension of the solder jumper . . . . .	43
42	Latches of the plate system . . . . .	46
43	Balancing weights . . . . .	47
44	Inner belt tension adjustment . . . . .	47
45	Belt cover screws . . . . .	48
46	Motor mount screws . . . . .	49

## List of Tables

1	System Requirements for Rotational Casting Machine . . . . .	2
2	Bi-axial rotation value analysis . . . . .	5

3	Value analysis of Stepper and BLDC Motors . . . . .	5
4	Value analysis clamping solutions . . . . .	7
5	GPIO Definitions . . . . .	32
6	Most important states in the FSM . . . . .	34
7	Variables in each preset . . . . .	35
8	Budget overview . . . . .	38
9	Test parameters . . . . .	40
23	Gantt chart . . . . .	54

# 1 Introduction

Soft robotics has proven to be a valuable alternative to traditional robots made of metals and plastics, offering systems that are both lightweight and inherently compliant. These characteristics allow soft robots to interact with delicate environments more safely and effectively than rigid designs can. This makes them particularly well suited for applications where robots work in close contact with humans or other sensitive systems, such as biomedical devices, wearable technologies, and prosthetics. In these areas, soft robotics is enabling new capabilities and improving existing solutions.

The compliant behavior of soft robots is largely enabled by a different class of actuators that rely on hollow silicone components which deform under internal pressure. This places specific demands on fabrication methods, particularly the ability to produce complex internal geometries with controlled wall thickness. Such precision is essential for achieving predictable and repeatable deformation. Current manufacturing techniques often rely on multi-part molds and casting processes, which require intricate assembly steps and introduce seams or weak points. While sacrificial cores address some of these challenges, they are typically costly, time-consuming, and still require openings for removal. As a result, fabricating seamless, complex hollow structures remains a significant obstacle in soft robotics.

Rotational casting offers a more efficient solution by enabling the direct formation of hollow silicone structures in a single step. This is achieved through continuously rotating molds that spread soft silicone uniformly around the interior. This eliminates the need for sacrificial cores or tedious and failure-prone joining processes. To better control the distribution of material around the mold interior, the rotation on different axes needs to be decoupled and controlled independently.

Rotational casting machines are widely used in industries producing hollow, thin-walled plastic products such as containers, ornaments, helmets and kayak hulls. These machines are not well suited to the fabrication of soft actuators, especially in a research environment. This report will focus on developing this missing piece, a rotational casting machine dedicated to soft actuator fabrication in a research environment.

All development aspects of the machine, such as the design, fabrication and testing will be discussed, starting with a detailed set of requirements. Based on these requirements, a conceptual design is developed through functional decomposition and value analysis. This conceptual design is subsequently translated to a full mechanical, electrical and software design that can be constructed. Finally, some preliminary testing is done on the resulting machine to assess its functionality and propose refinements for eventual successors.

## 2 Requirements

From the initial problem statement a set of requirements (see table 1) was derived. The most important requirement is that the machine has two independent speed-controlled rotation axes. This gives the user more control over the properties of the final molded part. The required rotation speed for the frames was determined by looking at similar machines [2] that are already on the market.

In consultation with the commissioning supervisors, several requirements regarding the size and weight of the molds that the machine should be able to hold. Safety is of course also a priority, so several requirements have been formulated to ensure the final design does not endanger its users or environment. Lastly, some requirements were added to ensure user-friendly and fast operation, cleaning and maintenance.

Requirement	Description
R01	The rotational speed of each axis shall be independently adjustable.
R02	The machine shall accommodate molds of various sizes and weights, which must be securely fastened. The maximum mold size shall be 30×30×30 cm.
R03	The machine shall accommodate molds weighing up to 5 kg.
R04	The rotational speed of both axes shall be adjustable by the operator, within a range of 1 to 30 rpm, to suit different materials and designs.
R05	The machine shall automatically stop after a predefined curing time, which can be set between a few minutes and a maximum of 24 hours.
R06	The system shall allow for minimal delay between mixing and rotation initiation. This requires a quick-clamping mechanism and an intuitive user interface for speed adjustment.
R07	The system shall include material presets.
R08	The design shall allow for easy cleaning and maintenance, particularly in areas where materials might spill.
R09	The materials in areas where materials could spill shall be resistant to ethanol, acetone, and isopropyl.
R10	The system shall provide an interface for setting curing time, independent axis speeds, and temperature control (if applicable).
R11	The machine shall be designed to fit on or under a standard worktable by having a footprint of at most 70×70 cm.
R12	The system may include a controllable heating mechanism to accelerate the curing process, with configurable temperature up to 60°C.
R13	The machine shall feature an emergency stop.
R14	All rotating components shall be enclosed to prevent accidental contact.
R15	The system shall include a mechanism that pauses rotation when the enclosure is opened.
R16	Electrical components shall be adequately insulated or enclosed.
R17	The system shall incorporate the necessary safety mechanisms for active components (e.g., motors, heating elements) to enable unsupervised operation.
R18	The target budget for the system is €500.

Table 1: System Requirements for Rotational Casting Machine

### 3 Conceptual design

To systematically and efficiently design a machine that meets all specified requirements, a functional decomposition conducted. From the list of requirements, four non-trivial functions were identified. The following subsections describe these functions, detail (at most the two best) possible solutions to realize them, and compare alternatives to select the best suited solutions.

Prior to defining the functional structure, examples of existing rotational casting machines were examined, in both industry and hobby environment. These references aide the design by providing common design approaches to some functions, as well as proven solutions.

Functions that are straight-forward and not critical to the core functionality of this particular machine are not included in this conceptual design, but will be briefly discussed in later sections describing the physical design.

#### 3.1 Bi-axial rotation

The most fundamental function of a rotational casting machine is rotating the mold. In this case, rotation is required around two perpendicular, independent axes. Strictly speaking, this function comprises of two sub-functions, one being providing a structure with the necessary degrees of freedom and the second being the transmission of motion within this structure.

However, the first is very straightforward, as demonstrated in existing machines that virtually all use the same approach of a gimbal-like arrangement of two concentric frames that can rotate in perpendicular axes [1, 2, 3, 4]. Since most machines, including this one, are designed with a cubic working volume in mind, these frames are typically square. This type of construction is shown in Figure 1. This construction is simple, effective, cheap and easy to realize making it used in industrial and hobby machines alike. This approach will thus be used, and the remainder of this section will discuss the second subsection.



Figure 1: Example of a bi-axial rotating frame construction used in an industrial machine [1]

However, transmitting motion from a power source to these frames is not trivial, and many solutions are possible and have been realized. They can be separated in two groups, using either (quasi)direct drive or using a form of transmission.

##### 3.1.1 Direct drive

In what is referred to as a direct drive setup, one motor is stationary and drives the outer frame. The second motor is attached to this outer frame and drives the inner frame. A small set of belts is

sometimes used to provide some reduction and a more compact motor mounting, meaning the setup is not strictly a direct drive. The key distinction from other systems is that one motor is mounted on a moving frame.

This setup is used in both industrial [1] (see also Figure 1) and hobby-oriented machines [2], as it is suited for both small machines typical to the hobby environment and medium to large sized machines used in industrial setups. For large machines with big motors, keeping all motors stationary is often preferred.

The main advantage of this approach is the limited amount of added components. This enhances reliability while also making the design, construction, and maintenance easier. The downside of one motor being mounted to a moving frame is the increased rotating mass. For this particular machine, this also means one motor is unavoidably in the heated zone which most common cheap motors are not designed for.

### 3.1.2 Transmission

Another common approach is to use a transmission on the outer frame to transmit rotational motion from two stationary motors to the rotating frames. This transmission often includes a combination of bevel gears and chains or timing belts [4], an example is presented in Figure 2. For smaller machines designed for lighter molds, this setup can be simplified to use a single timing belt that wraps around the outer frame [3].



Figure 2: Example of transmission based rotational casting machine

This setup keeps both motors stationary, reducing moving mass and keeping them outside the heated environment. The lack of a motor on the outer frame and more flexible motor mounting options also allows for a more compact design. This comes at the cost of increased components potentially reducing reliability and increasing maintenance. For a smaller machine with the aforementioned simplification to a single timing belt, this downside is much less significant.

### 3.1.3 Comparison and value analysis

Both approaches clearly have their strengths as demonstrated by existing machines and the value analysis presented in Figure 2, but the transmission system scores significantly better. This machine also stands out among existing solutions with its heated environment. For this reason, keeping both motors out of this heat is preferred which makes a transmission system the better choice.

The compactness of this system is also very beneficial table space in the lab is valuable. Given the relatively small mold size, the transmission system can be simplified to minimize additional components and complexity.

	<b>Direct drive</b>	<b>Transmission</b>
Moving mass	- heavy motor	+ transmission components lighter
Added imbalance	- large due to motor	+ minimal
Heat influence on motors	- motor in heated area	+ external motors, not affected
Reliability	+ higher	- reduced due to extra components
Maintenance needs	+ minimal, easy	- belt replacement
Compactness	- less flexible motor placement	+ motor placement very flexible
<b>Total score</b>	<b>-2</b>	<b>+2</b>

Table 2: Bi-axial rotation value analysis

### 3.2 Generation of rotational motion

To generate the necessary rotational motion, motors are necessary. For this machine electric motors are the most practical. Of all electric motor types, two were identified as particularly suitable in size, cost and power.

Apart from the criteria described above, another important characteristics for this application is torque at low speeds, as even with a reduction in the transmission the motors will turn quite slowly. The motors should also be sufficiently quiet, as the machine will be placed in a lab with a relatively quiet environment. Controlling them should be easy, and detecting abnormal states to ensure safety is also important as evident from requirement R17. Lastly, long lifetime and low maintenance are also desired.

Two common motor types that fail to meet these requirements are DC motors, because of their brushes that are noisy and have limited lifetime, and AC induction motors because scalar control is not very stable at low speeds and Field Oriented Control is expensive.

Two motor types that meet these requirements are BLDC motors and (hybrid) stepper motors. These are both very common motors in machine tools, so a detailed description is omitted here. The main benefit of stepper motors is their excellent torque and control at low rpm, while the BLDC motor excels at quiet operation and long lifetime. Table 3 presents a more detailed comparison between them in the form of a value analysis on the important characteristics for this application.

	<b>Stepper Motor</b>	<b>BLDC Motor</b>
Price	+ cheaper	- more expensive
Torque (at low speed)	+ high torque	- medium torque
Control (open loop)	+ position and speed control	- only speed control
Lifetime	+ high	+ very high
Noise and vibrations	- more vibrations	+ low vibrations
Drivers	+ good safety features	+ good safety features
<b>Total score</b>	<b>4</b>	<b>0</b>

Table 3: Value analysis of Stepper and BLDC Motors

For this application it is thus clear that hybrid stepper motors are the better choice. Their downside of higher noise and vibrations can be reduced by using high quality drivers, which also have plenty of safety features that will go a long way in making the moving components safe in autonomous operation. More details on the chosen drivers and their features are presented in Section 5.1.

### 3.3 Connecting the mold

The requirements for this function are simple; the molds should be mounted securely and the mechanism to do so should be easy to use. Ease of use means a system that is flexible to adapt to different mold sizes and shapes with minimal adjustments and that is quick to use as the pot life of the used elastomers is limited. Strictly speaking there is no requirement to be able to fit multiple different molds in the machine, but it would enhance its capabilities.

When looking at existing solutions, none of these fit the bill. Industrial machines are set up for series production, not flexible mounting and users are expected to develop their own solution specific for the mold (types) they want to use. Consumer/hobby machines use all kinds of systems that focus either on secure mounting or ease of use but rarely both. Examples of the former include parallel plates that clamp the mold but are tedious to adjust, while examples of the latter are holding molds in various rubber band contraptions that are not secure.

Quite some different mold mounting mechanisms were considered, here only the best two contenders that remained compelling will be discussed.

#### 3.3.1 Clamping bar

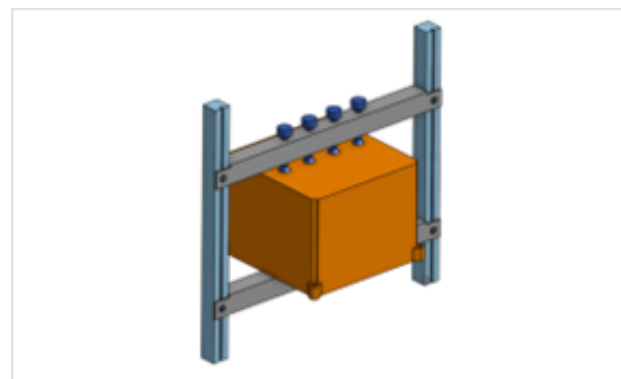
Firstly, an option is to take inspiration from the parallel plates often seen on hobby machines as illustrated in Figure 3a and try to address some of its problems.

The parallel plates are not very easy to use, as especially for larger machines and small molds it can be hard to position a small mold in the middle of the plates whilst closing the plates. They also lack some flexibility due to the fact that for a secure clamping flat surfaces on either end of the molds are needed, which requires adapting current molds that often have bolts sticking out of either end. They are also not capable of clamping multiple different molds, and the two large plates add considerable moving mass to the system.

These issues could be addressed by changing the plates to parallel bars as shown in figure 3b. This makes it much easier to position molds between them as there is more access from all sides. By integrating smaller clamping elements in one of the bars no large flat surfaces are needed, just a couple of flat spots. This would also allow to roughly position the bar with a fast mechanism and clamp with a finer and more precise mechanism. To some extent multiple molds could be fit but with quite some constraints still. The moving mass is also greatly reduced. The clamping however is arguably less secure, as the contacting areas are smaller.



(a) Example of parallel plate system



(b) Proposed camping bar system

Figure 3: Proposed alternate clamping system

#### 3.3.2 Perforated plate

Many mounting solutions in machine tools make use of grids of mounting features, often (threaded) holes. This principle could be used by making a plate with adjustable height (to balance the mass)

with a grid of holes as illustrated in Figure 4. A mold would then be secured by a number of bolts through the mold and the plate, making for the most secure mounting of all options.

This approach puts very limited constraints on the mold outer geometry, as the only requirement is some bolt holes that align with the grid. Multiple molds can easily be fitted without additional constraints.

The drawback of this system is that bolts are needed, which takes time and can be tedious to fasten. However this is not a big issue. Note that most molds already contain bolts to clamp the two sides together, so this would only add constraints to their position. By making the plate removable, fastening the molds to it would be a lot easier and less tedious with access from all sides.

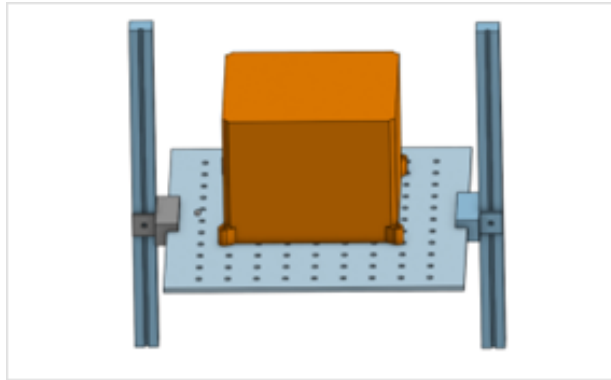


Figure 4: Illustration of perforated plate

### 3.3.3 Comparison and value analysis

In terms of clamping the perforated plate is without a doubt safer, as it is form closed as opposed to the force closed clamping bar system. In terms of ease of use they seem similar, as it is a somewhat subjective benchmark it is hard to say which is better. The added inertia is likely lower for the clamping bar. To balance, the perforated plate allows easier height adjustment and also adjustment in the plate plane, though the latter is quite tedious and in discrete increments. The clamping bar only provides height adjustment and requires adjusting more elements to accomplish this.

A detailed comparison is made through a value analysis shown in Table 4. As the perforated plate seems has a clear advantage compared to the clamping bar, it is the preferred approach.

	<b>clamping bar</b>	<b>Perforated plate</b>
Ease of use	- two adjustments	+ single adjustment
Constraints on mold	- flat and parallel surfaces	- bolt holes
Strength of clamping	- force closed	+ form closed
Supports multiple molds	- yes, but with a lot of extra constraints	+ yes, but on the same plate
Position adjustment	+ continuous in 3D	- 1D continuous, 2D discrete
<b>Total score</b>	-3	1

Table 4: Value analysis clamping solutions

### 3.4 Heating

Elevated temperatures can significantly decrease curing times of elastomers commonly used for the fabrication of soft robot components [5]. As a rule of thumb, the curing time is halved for every 10°C. As curing times are often several hours, this reduction leads to significantly shorter cycle times. As the machine should be enclosed for safety, heating this enclosed environment makes sense.

Molds are usually FDM 3D printed out of PETG polymer, which has a heat deflection temperature of between 65°C and 75°C depending on the material formulation. This sets the upper limit for the

ambient temperature in the machine, as the molds should not deform during casting.

The most important requirement for the heating mechanism is safety. The mold should also be heated as equally as possible, to avoid thicker walls in hotter areas due to the increased curing rate. The heater should also be compact. Besides this, cost and ease of implementation are also relevant as this is not a core function of the machine.

With the above requirements and the only energy source of the machine being electric, a PTC heater was the only viable solution found. It is a form of joule heating where a positive temperature coefficient resistance (PTC) is used. This means that as temperature increases, the resistance will increase, decreasing the dissipated heating power under constant voltage as  $P = V^2/R$  so a maximum temperature can be engineered into the material of the resistor. This inherent temperature limit makes it one of the safest forms of electric heating. They are often combined with a ventilator to use forced convection to increase thermal transfer to the environment.

PTC heaters are very affordable and available in many different sizes, making them easy to integrate into the machine. Heating the air surrounding the mold which is constantly mixed by the movement of the rotating elements should ensure sufficiently even heating.

## 4 Mechanical design

### 4.1 Frame

The main purpose of the frame is to provide a rigid base to which all the components can be easily connected.

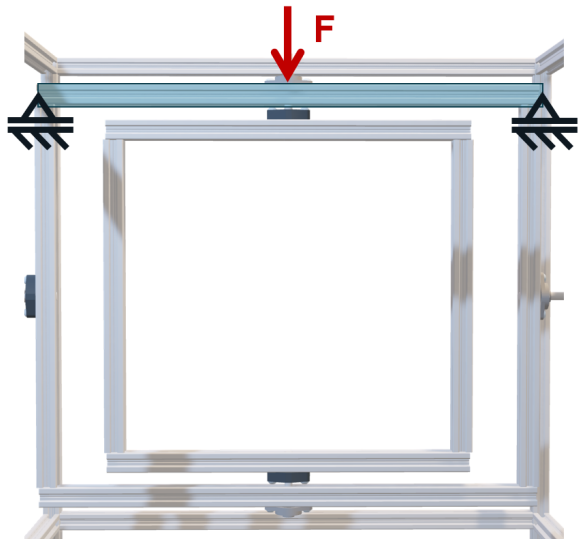
#### 4.1.1 Geometry

The geometry of the frame was mainly determined by the maximum mold size the machine should be able to accept. Requirement R02 in section 1 states that the maximum mold size is 30x30x30 cm. The inner rotating frame was thus this 30 cm plus some clearance and some space for the rails of the mounting system. This came out to be a rectangle with an inside dimension of 330x313 mm. The outer rotating frame is a bit wider than it is tall. This is because it needs to clear the diagonal of the 30x30 cm mold due to its rotation. This came out to be an inside dimension 466x383 mm.

Finally the frame for the enclosure is just big enough to leave a couple of centimeters of clearance to the rotating components and has an outside dimension of 570x550x615 mm. There is also a space with a height of 60 mm underneath the main enclosure to house the electronics.



(a) CAD drawing of the frame



(b) Maximum load case

Figure 5: Frame

#### 4.1.2 Material

There are many different options for the material of the frame such as aluminium extrusions, steel tube, or even wood. Aluminium extrusions were chosen because they are light weight while still being rigid structural members. They are easier to process than steel while being more rigid than wood, and are more chemically resistant than the alternatives. Their modular design provides ample options for mounting and assembling of the different components of the frame.

Aluminium extrusions come in many different sizes and shapes. 20x20 mm Aluminium extrusions with 6 mm side T-slots were chosen based on the maximum load case scenario for a mold of 5 kg. Due to the slow rotation speeds the dynamic load on the system is negligible compared to the static load due to gravity. Figure 5b shows the frame member that experiences the most stress as a result of this static load. The load in this case consists of a mold of 5 kg plus a 2.5 kg for the inner frame, mounting system and other components. The beam is modeled as being simply supported on either side as the

single screw connection will not deliver large reaction moments.

This load is distributed evenly over the top and bottom member of the outer frame, and results in a force of 38 N on each member. Using simple beam theory gives the following results: A maximum stress of 7 MPa, well below the material limits of aluminum and a maximum deflection of 0.22 mm which is an allowable deflection for this application. This makes the 20x20 mm profiles a good balance between strength on the one hand and cost and weight on the other for this use case.

#### 4.1.3 Connections

To connect all the frame members a bind joining technique was used, as it is secure whilst needing minimal extra parts adding to assembly time and cost. The ends of each member of the frame were tapped with M6 threads. By sliding a socket button head cap screw into the T-slots of the frame members and screwing these into into the threaded ends of the frame members a secure blind connection can be made. To tighten the cap screws a access hole needs to be drilled through one of the members so a hex key can access the screws. Figure 6 shows a drawing of the blind joining technique used in the frame. These connections where secured using Loctite® thread locker so they wont vibrate lose over time.

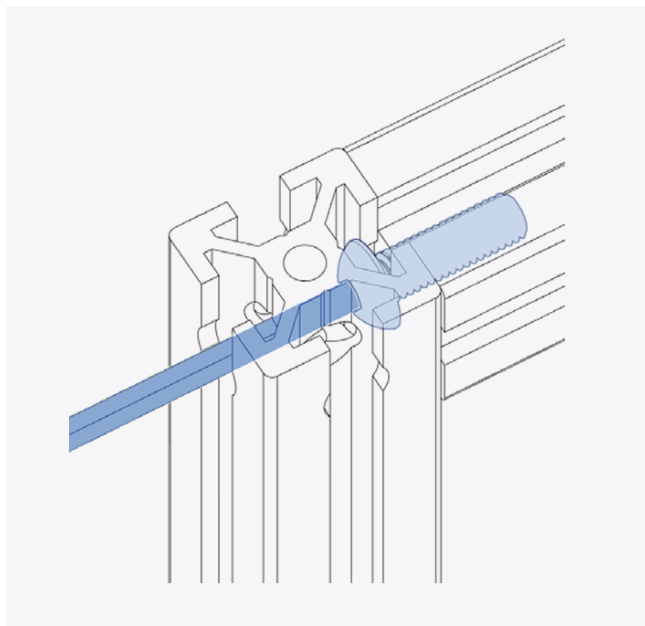


Figure 6: Blind joint technique used on the frame

## 4.2 Kinematics

The machine has two rotations axis that are capable of moving independent of each other. This is realized by two stepper motors and a transmission system made from belts and pulleys as decided in the conceptual design.

#### 4.2.1 Kinematic relations

Because of the choice for a transmission system instead of direct drive the rotation speed of both frames is no longer simply the rotation speed of the driving motor, instead the two ratios speeds are kinematically coupled to one and other. Because of this the motors need to compensate for this kinematic relation.

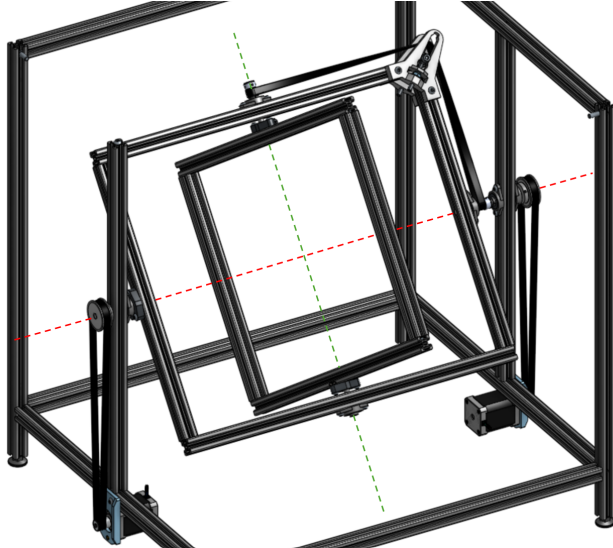


Figure 7: Rotation axis of the machine

Both motors are fitted with a 3 to 1 belt reduction in order to get more torque out of the motors as they are only used at low rpm. The relation between the rotation speed of the outer frame motor  $\omega_{M,o}$  and the outer frame rotation  $\omega_o$  (around the red axis) is simply the belt reduction. The relationship of the inner frame rotation  $\omega_i$  (around the green axis) and the inner frame motor  $\omega_{M,i}$  is more complicated due to the relative motion created by the outer frame rotation  $\omega_o$ .

$$\begin{aligned}\omega_o &= \frac{1}{3} \cdot \omega_{M,o} \\ \omega_i &= \omega_o - \frac{1}{3} \cdot \omega_{M,i}\end{aligned}$$

Transforming these equations into motor speed in function of the desired frame speed gives:

$$\begin{aligned}\omega_{M,o} &= 3 \cdot \omega_{M,o} \\ \omega_{M,i} &= 3 \cdot (\omega_o - \omega_i)\end{aligned}$$

There are a couple of interesting observations to be made about these equations. First of all if both frames rotate at the same speed the required motor speed for the inside motor becomes zero. This means the motor needs to have high holding torque and ideally position control to stay at a fixed position, both are no problem for the stepper motors. If the rotation speed of the inside frame is zero the speed of the inside motor needs to match that of the outside motor. Thus the bigger the difference between the inside and outside frame the faster the inside motor has to turn. This reaches a maximum of 180 rpm if the inside frame rotates at -30 rpm and the outside frame rotates at 30 rpm.

#### 4.2.2 Transmission

The transmission for the inside frame consist of two parts firstly the 3 to 1 belt reduction on the outside of the frame and secondly the corner belt transition on the outside of the outer rotating frame. For the outside frame it is only the 3 to 1 belt reduction. The type of belts and pulleys chosen for the transmission is the 9 mm GT2 system. These parts were readily available in many sizes at low cost due to their use in consumer 3D printers, which made them very affordable. They are not heavy duty, but strong enough to handle the torque.

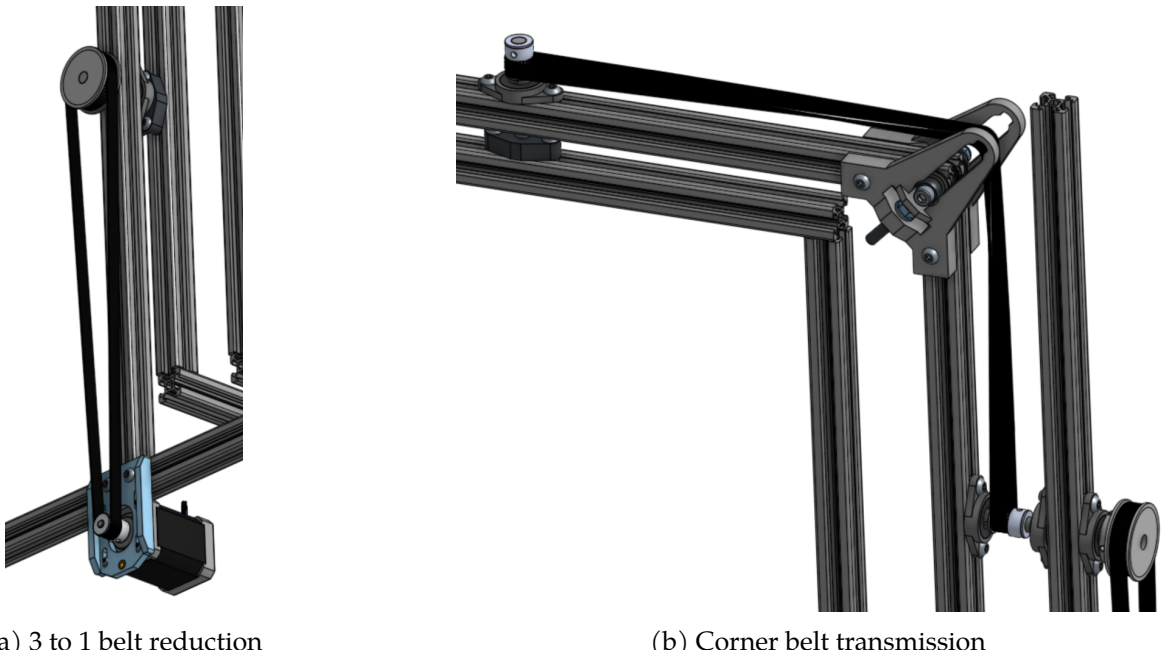


Figure 8: Belt transmissions

The 3 to 1 belt reduction consist of a 20 teeth pulley clamped directly on the 5 mm shaft of the motor and a 60 teeth clamped a 8 mm axle. The belt can be tensioned/de-tensioned by moving the motor up and down in the slots on the motor mount before tightening it down.

On the left on the machine the axle is supported using a single bearing blog connected to the frame and is rigidly connected to the outside rotating via a clamping block. On the right side of the machine the axle is supported by two bearing blocks to create a more rigid connection. This is needed because of the larger space required for the transmission system. This axle is also connected to the outer rotating frame with a bearing block so it can rotate independently of the outer frame. Figure 8a shows the transmission on the left side of the machine and 8b shows the transmission on the right side that is connected to the inside rotating frame.

The corner transmission consist of three part the two 20 teeth pulley and a roller guide that also servers a belt tensioner. The belt is twisted so it is able to make a 90 degree bend around the frame.

#### 4.2.3 Belt tensioner

The belt tensioner serves two purposes. It is the corner guide for the belt and it keeps tension on the belt. In figure 9 the CAD model of the belt tensioner is shown. This is a custom 3D-printed part which holds two eye bolts than can be adjusted in height using a captive nut.

It and all other custom components inside the enclosure are printed out of polycarbonate (PC 275 from Spectrum® filaments). Polycarbonate has excellent mechanical properties (high toughness and strength) and chemical and thermal resistance. It does not degrade under exposure to the proposed cleaning agents and has a heat deflection temperature of 150 °C which is more than sufficient. It is also possible albeit challenging to print on consumer 3D printers.

Through the two eye bolts is a large bolt around which is a stack of four flanged bearings spaced out by washers. These bearings are placed in such a way that they become flanged roller guides for the belts.

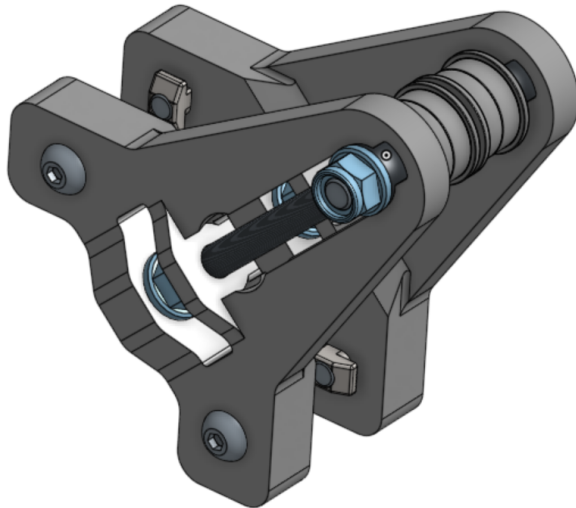


Figure 9: Belt tensioner

### 4.3 Motor selection

The exact torque requirements from the hybrid stepper motors will vary significantly depending on the mold weight, geometry and how well it is balanced.

To get an idea of the minimum torque, the inertia of the frames and the mold can be calculated using basic formulas for thin rods, cubes and the parallel axis theorem. Assuming the mold is a 30 cm cube weighing 5 kg and the inner frame is perpendicular to the outer frame so its inertia contribution is as large as possible, this results in a moment of inertia of  $0.09 \text{ kgm}^2$  around the outer rotation axis and  $0.22 \text{ kgm}^2$  around the inner rotation axis. Assuming the frames accelerate to 30 rmp in 30 s and there is a 3:1 reduction in the transmission, this requires a torque of 8 Ncm and 3 Ncm on the outer and inner frame respectively. To keep integration and tuning simple, both motors will be identical even though they have different torque and speed requirements.

Significant torque contributions that were neglected in this calculation are friction, imbalance and inertia of additional components (perforated plate, transmission elements). So a significant safety factor of 3 seems appropriate, making the torque requirement 24 Ncm. The maximum rpm of the motors accounting for the transmission and kinematics is 180 rpm (inner motor frame).

One of the most common and thus cheap mid size stepper motor sizes is a Nema 17 motor, making it a straightforward starting point. The motor windings can be connected in different ways, which changes the torque and efficiency of the motor. Bipolar is generally the most efficient and powerful and only slightly more expensive, making them the better choice. A suitable candidate is the 17HE24-2104S Nema 17x60mm bipolar hybrid stepper from Stepperonline.com that produces 60 Ncm holding torque at 2.1 A phase current and keeps this high torque up to 180 rpm as shown on its torque-rpm visible in Figure 10.

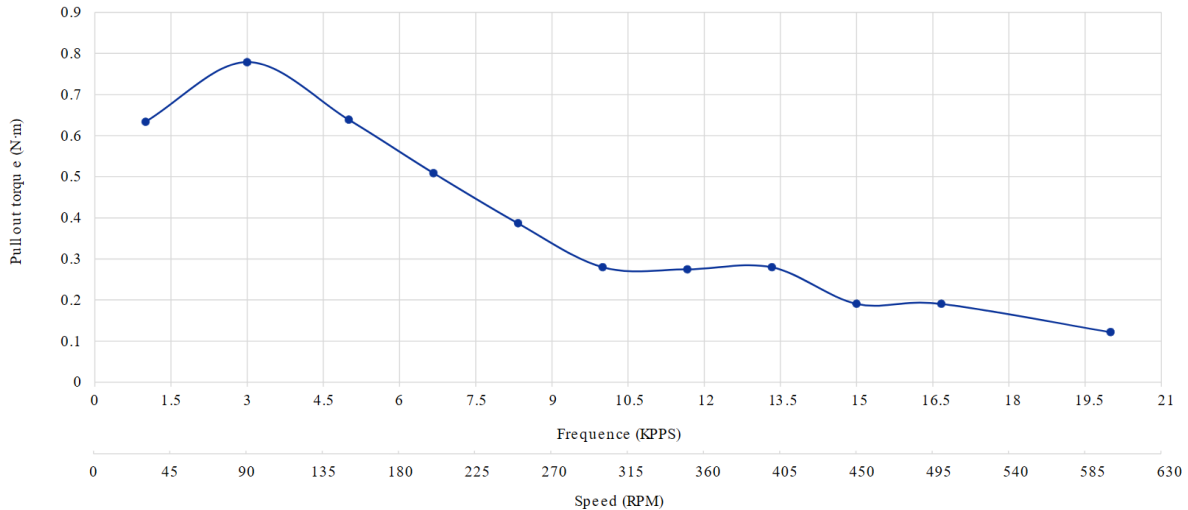


Figure 10: 17HE24-2104S Torque graph

The drivers whose selection will be discussed later can only supply a maximum phase current of 1.2 A, and since torque is proportional to phase current only about 30 Ncm of torque will be available which is still sufficient. The reason a motor with smaller maximum phase currents was not selected because the examples found did not maintain a high torque in the 0-180 rpm range.

#### 4.4 Mounting system

The mounting system consists of a removable plate with a grid of holes, mounted in two sliders. The sliders are mounted on the vertical members of the inner frame with sliding brackets to make it possible to adjust the height of the plate via two handles. An overview with labeled components that will be discussed in this section is shown in Figure 11. All the custom components visible as mentioned before were 3D printed out of polycarbonate.

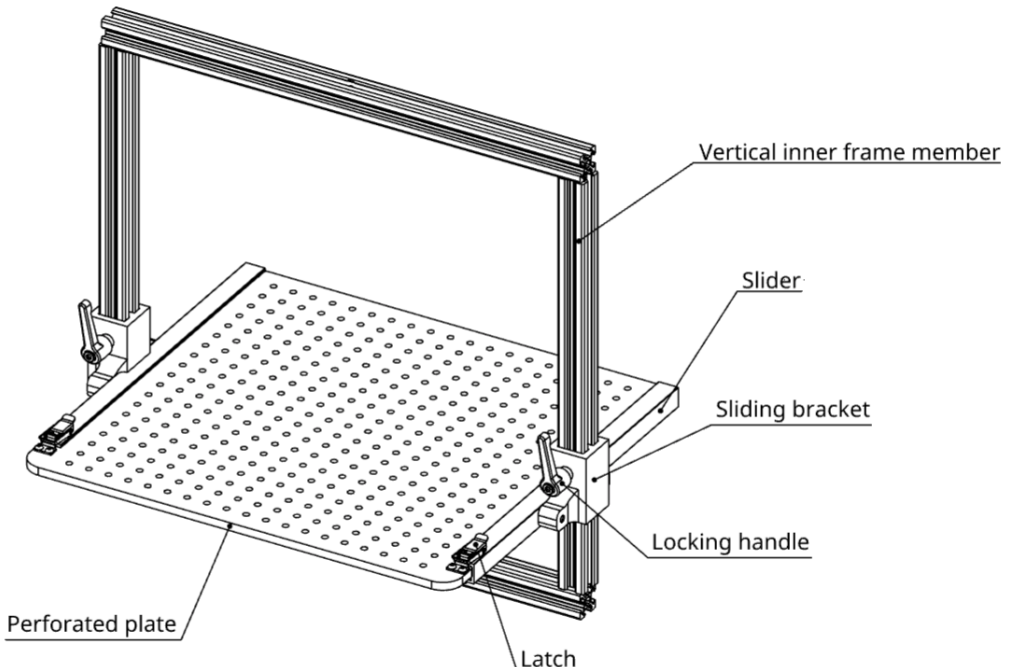


Figure 11: Plate system overview

#### 4.4.1 Plate

For the plate material, two options were considered: polycarbonate and aluminium. Polycarbonate is the most suitable polymer, as it boasts excellent toughness, temperature and chemical resistance and is easy to work with. It also has a slightly higher strength to weight ratio compared to aluminium and is cheaper. Polycarbonate is also transparent, so manipulating hardware on either side of the plate to mount a mold is easier.

Aluminium also has the necessary mechanical properties and chemical and thermal resistance. The advantage of aluminium is higher stiffness to weight ratio. For a 5 kg mold, both materials are more than strong enough and the plate thickness needed depends thus mostly on stiffness. This means the aluminium plate would be lighter than one made of polycarbonate.

As the budget and the fabrication tools available are limited, polycarbonate was chosen. The stiffness is also not critical in this application and as evident from the motor selection there is plenty of torque available so a heavier plate is not detrimental. The transparency will also be great in reducing the hassle of mounting molds.

For the mounting pattern, a grid spacing of 15 mm was chosen as a balance between maintaining plate strength and providing flexible mounting options. As the fasteners currently used in the lab for closing molds are mostly M3 and M4, the hole diameter chosen was 4.5 mm so both can easily be used (ideally with washers for M3).

To determine a suitable plate thickness offering sufficient stiffness at a reasonable weight and price, an FEA simulation was performed in Autodesk Fusion360 as analytical solutions for a plate with holes were not found. The actual load case will greatly depend on the mold size and geometry and rotation speeds, so the purpose of this simulation is to provide proof that even in a worst-case type of scenario the plate thickness is sufficient. For the plate this is a large load acting in a small area in the center.

For the constraints, two sides of the plate were fixed. The meshing was done automatically. The load from the 5 kg mold was simulated with a safety factor of 2 in part to account for dynamic unbalance resulting in a force of 100 N which was distributed on the nine most central hole edges. The plate's own weight was also added as load. For a 6 mm thick plate, this resulted in a maximum total displacement of 1.54 mm which was deemed reasonable. The total displacement results along with the mesh and load case are shown in Figure 12.

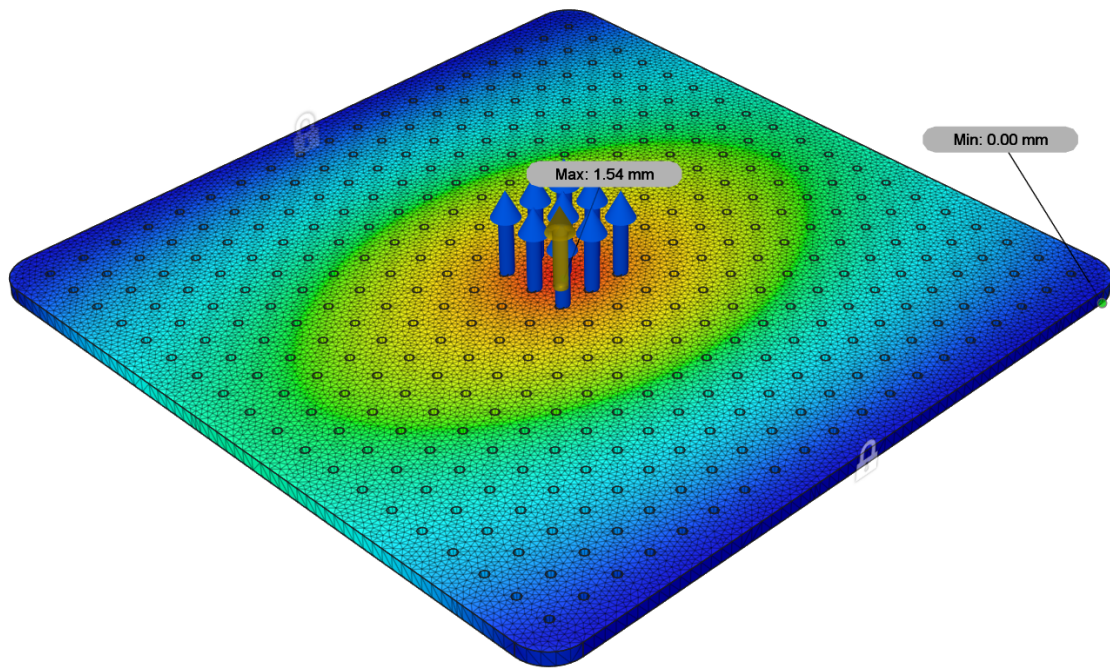


Figure 12: Plate FEA results

#### 4.4.2 Sliders

An aluminium C channel acts as the main structural member of the sliders. An insert was used to make sliding the plate in and out easy whilst also eliminating play with compliant clamps. The plate will be secured by clamping it against a stop with a latch on either profile. A latch was chosen as it is an easy to use and toolless mechanism that can be quickly secured or released. A close up of the slider system is shown in Figure 13.

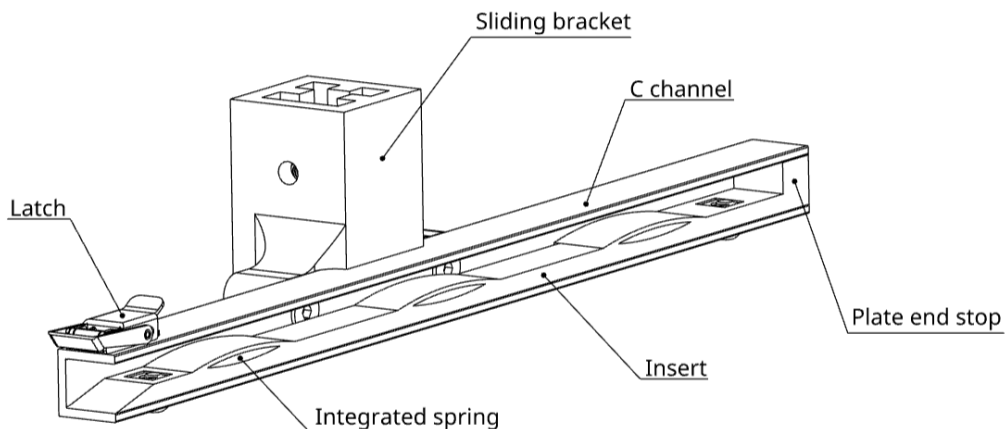


Figure 13: Slider overview

The selected C-channel has a wall thickness of 2 mm which should be plenty strong and outer width of 15 mm to leave space for an insert under the plate.

The insert mounted in this channel has a ramp in the front to guide the plate into the slider, three integrated springs to eliminate play and an end stop that the plate is clamped to with the latch mounted on top of the C channel. The integrated springs consist of a leaf type spring integrated into the slider. Its exact dimensions were fine-tuned in a couple iterations to achieve a good balance between requiring not too much force to insert the plate whilst also clamping the plate sufficiently strong to eliminate

play between the plate and the slider. This insert allows to have a large clearance between the plate thickness and the slider slot width making the plate easier to insert whilst preventing it from moving once the frames start rotating.

The latch needs to be strong to hold the plate whilst being small enough to fit on top of the 15 mm C channel, significantly reducing the suitable latches. It is also important that vibrations due to unbalances do not accidentally open the latch. The tight-hold draw latch 1794A51 from McMaster-Carr fits these requirements as it is small but rated at 890 N which is more than sufficient. It also has integrated compression springs that prevent vibrations from causing accidental release.

#### 4.4.3 Sliding bracket

The sliding brackets holding the sliders to the vertical inner frame members is shown in Figure 14. They can be fixed or loosened with a nylon adjustable handle that rotates freely when lifted. This free-rotating mechanism allows for large adjustments even when the slider block full rotations of the handle. It also allows the handle to be positioned perfectly vertically when tight so it does not hit anything during operation. Tightening the handle pulls on an M5 sliding nut inserted in the aluminium profile.

Two M5 square nuts are inserted into the 3D printed part to make fastening the sliders to the bracket with two M5x16 screws really easy. Their square shape makes for a large contact surface to the part on all sides.

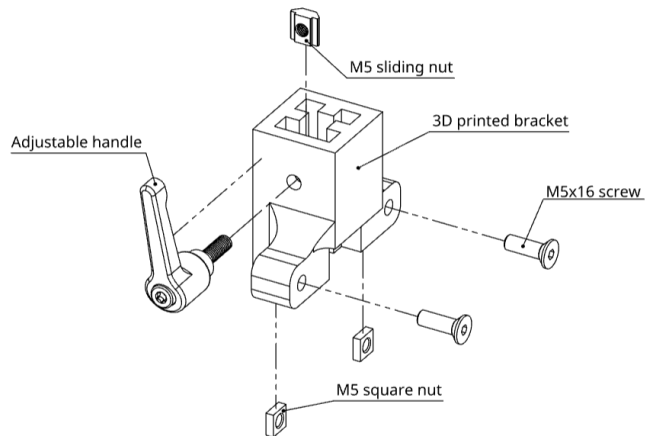


Figure 14: Sliding bracket

#### 4.5 Enclosure

The main purpose of the enclosure is to keep in the heat and to shield all the rotating/electrical component for safety as described in requirements R14 and R16. The enclosure also needs to be resistant to all chemicals used to clean up any silicone spills as described by requirement R9.

The main qualities that a material for the enclosure needs to have are chemical resistance, impact resistance to protect from rotating components and being able to withstand a heated environment up to at least 60°C. There are many different materials that have these qualities but in the end two materials were chosen for the enclosure. For all panels except the door 3 mm thick high-density polyethylene (HDPE) was chosen. This was mainly due to it being by far the cheapest option and easy to work with. For the door a 4 mm thick polycarbonate plate was chosen for the simple fact that it needed to be transparent.

The door of the enclosure was also fitted with magnetic door latches to keep the door closed as well as a limit switch detecting if the door is opened. This will stop the rotation as required by requirement R15. Since the enclosure is quite dark on the inside it is also equipped with a LED-strip which turns on automatically when the door is opened or any button is pressed on the interface so the process

inside can be inspected. Lastly a custom 3D-printed casing is placed around the belts so they can't be touched. This housing is printed out of ASA, a polymer with good thermal and mechanical properties that can withstand the needed cleaning chemicals.

Other enclosure parts such as the interface housing and hinges were also 3D printed out of ASA. A long LED strip is mounted in the top of the enclosure on brackets that snap into the aluminium extrusions to provide some protection and put the LEDs on a better angle. The LEDs are needed as the mostly black enclosure is very poorly lit by ambient light making process inspection very challenging. These brackets were printed out of transparent PETG, which has inferior mechanical and thermal properties to ASA but is transparent.

This results in the enclosure design shown as CAD model in Figure 15 together with a picture of the final result shown in Figure 16.

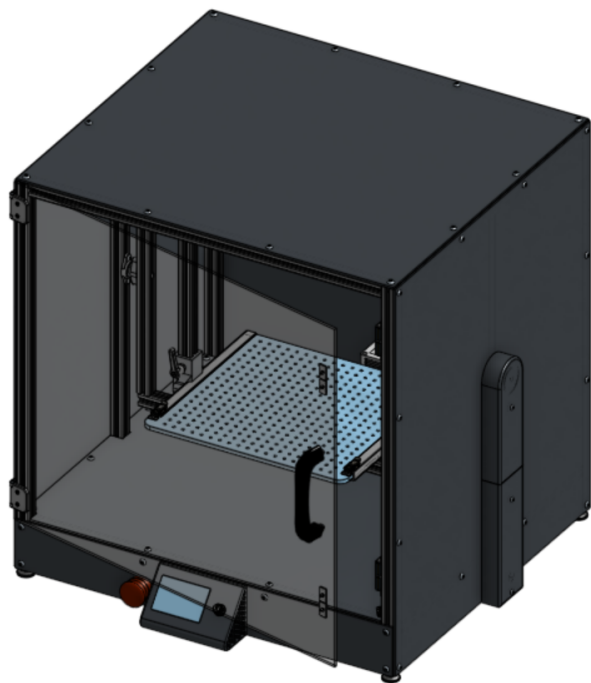


Figure 15: Enclosure

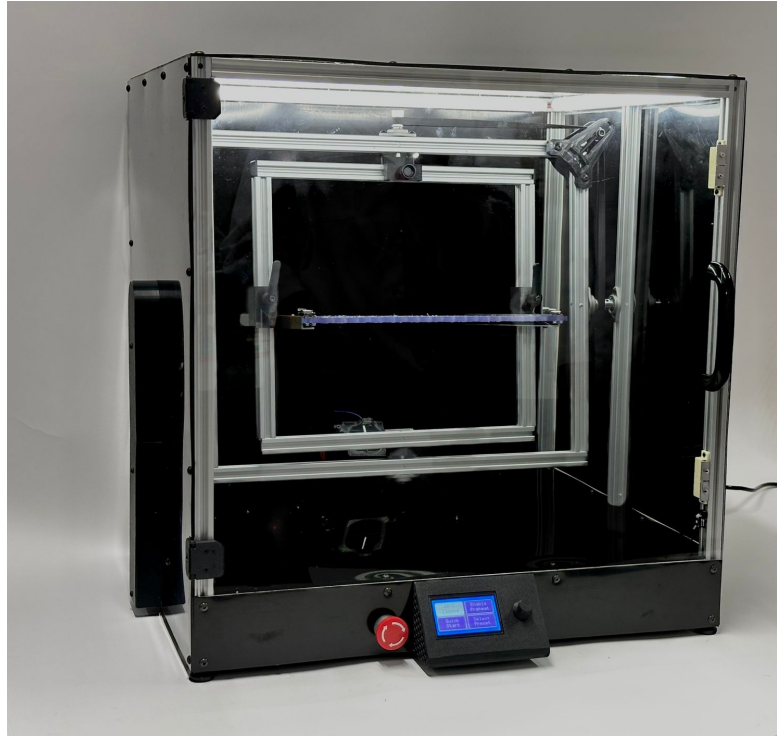


Figure 16: Assembled Machine

## 4.6 Heater

### 4.6.1 Dimensioning

To determine the required heating power, a thermal model of the machine was developed. A full CFD model was out of the scope of this project, as heating is not a critical function. Still, some calculation is needed to make an informed decision on the heater specifications.

To simplify the machine, it is modeled as an isothermal cuboid, cooled by natural convection. In this way the complex turbulent flow around the rotating plates and the forced convection of the fan through the heater is neglected, and the heater is modeled as a distributed heat source in the cuboid. This simplification allows to use Nusselt correlations for isothermal cuboids cooled by natural convection [6].

To model the losses to the environment, a resistive network is used consisting of a conductive and convective resistance in series. The conductive resistance represents conduction through the enclosure plates, while the convective resistance models the natural convection around the cuboid. The plates are modeled as if they are all 3 mm HDPE as different plate thermal resistances would render the isothermal assumption invalid and the HDPE is a worse insulator so this build in a (very little) safety factor.

The system is modeled as a lumped thermal mass subjected to a constant heat input  $Q$  and energy losses through conduction and natural convection. The lumped body temperature  $T$  evolution is thus governed by an energy balance:

$$C_{tot} \frac{dT}{dt} = Q_{heater} - \frac{T - T_{ambient}}{R_{tot}}$$

where:

- $C_{tot} = C_{air} + C_{Alu}$  is the total thermal capacity, combining the heat capacities of the enclosed air and aluminum components ( $C = m \cdot c_p$ )

- $R_{tot} = R_{cond} + R_{conv}$  is the total thermal resistance, including conduction through HDPE ( $R_{cond} = \frac{t}{kA}$ ) and temperature-dependent natural convection to ambient air,
- $R_{conv} = \frac{1}{hA}$ , with  $h$  computed from the Nusselt number correlation for free convection around cuboids [6]
- $T_{ambient}$  is the ambient temperature of 20°C

The convective heat transfer coefficient is calculated using:

$$h = \frac{Nu_{\sqrt{A}} \cdot k}{\sqrt{A}}$$

where  $Nu_{\sqrt{A}}(T)$  is the Nusselt number with the root of wetted surface area as characteristic length calculated by the following correlation:

$$Nu_{\sqrt{A}} = Nu_{\sqrt{A}}^{\infty} + F(Pr) \cdot G_{\sqrt{A}} \cdot Ra_{\sqrt{A}}^{1/4}$$

where the diffusive limit can be found as

$$Nu_{\sqrt{A}}^{\infty} = \frac{3.192 + 1.868(L/H)^{0.76}}{\sqrt{1 + 1.189(L/H)}}$$

and with  $Ra$  the Rayleigh number and  $F(Pr)$  the universal Prandtl number function

$$F(Pr) = \frac{0.670}{[1 + (0.5/Pr)^{9/16}]^{4/9}}$$

and finally the body gravity  $G_{\sqrt{A}}$  function for cuboids

$$G_{\sqrt{A}} = 2^{\frac{1}{8}} \left[ \frac{0.625D^{4/3}W + H(D + W)^{4/3}}{(HW + HD + DW)^{7/6}} \right]^{\frac{3}{4}}$$

where  $D$ ,  $H$  and  $W$  are the enclosure depth, height and width respectively.

This nonlinear differential equation can be solved numerically for different heater powers  $Q_{heater}$ . An example of the resulting lumped body temperature for a heater with an output of 250 W is shown in Figure 17.

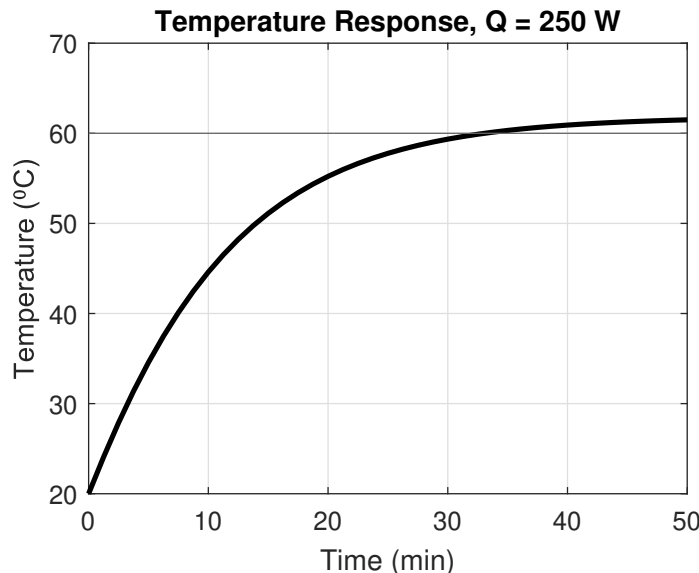


Figure 17: Simulated temperature inside the machine due to the PTC heater

Based on these simulation, a 250 W heater would be just sufficient. As quite some assumptions were made and the power supply had some power budget left, a 300 W heater was selected with an integrated fan.

#### 4.6.2 Integration

As an unevenly heated mold will lead to non-uniform wall thickness inside the molds due to faster curing, it is essential that the heating is as even as possible. For this reason, the heater should be placed centrally in the enclosure. To not obstruct access, it is positioned in the back and at the bottom as this is where the colder, less dense air that needs to be heated will naturally sink to as shown in Figure 18.

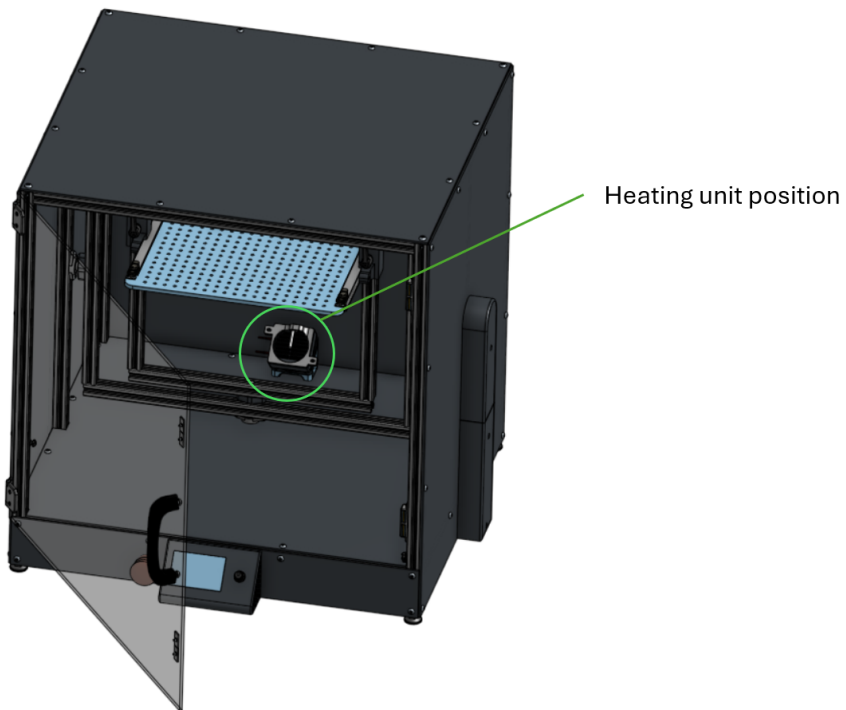


Figure 18: Heating unit position

The complete heating unit consists of some air intake/exhaust and support parts, an axial 60 mm 24 V fan, a PTC heating element, and a thermistor to measure the air temperature at the heater exhaust.

The intake and exhaust parts should provide mounting points to mount the heating unit to the bottom enclosure plate and prevent accidental contact with hot or moving parts. These parts were 3D printed out of polycarbonate, as it has a heat deflection temperature of 150 °C making it more than able to withstand the PTC elements temperature. It also has the necessary mechanical properties and chemical resistance.

The fan is placed before the heater in the colder air stream to prolong its lifetime. As the most important part about the temperature control in the enclosure is to elevate the temperature without melting anything, it makes sense to measure the hottest temperature and keep this under a certain limit. The hottest air is the one coming out of the PTC element, which is why the thermistor was placed there.

The first design of the complete heating unit is shown as version 1 in Figure 19. The intake was designed to prevent accidental contact with the fan and prevent silicone from accidentally dripping into the heating unit. The hot air is exhausted at the bottom to heat up all the colder air at the bottom of the enclosure.

During testing (see Section 8, it became clear the heating unit did not put out 300 W consistently. This was in part due to the airflow being too restricted at the intake and at the sharp 90° bend in the exhaust where a significant amount of air was reflected back up. Both of these obstructions together with the heat sink on the PTC element were too much for the low static pressure of the axial fan. As a result of this the heat from the PTC element was transferred to the enclosure air at a very reduced rate.

Another large problem was that the fan in general was underpowered and did not generate enough airflow to transfer the heat from the PTC element to the enclosure, even when unrestricted. As a result of this, the enclosure did not reach the desired temperature. As the fan was purchased as part of the PTC element to save costs, it had not been dimensioned properly.

To partly overcome these limitations and better heat the mold, the heating unit was redesigned. The hot exhaust was directed at the mold directly instead of at the bottom of the enclosure. This is less effective at heating the entire enclosure, but as it is only really the mold that needs to be heated this configuration is superior. Attention was taken to obstruct the airflow as little as possible. The result is shown as version 2 in Figure 19.

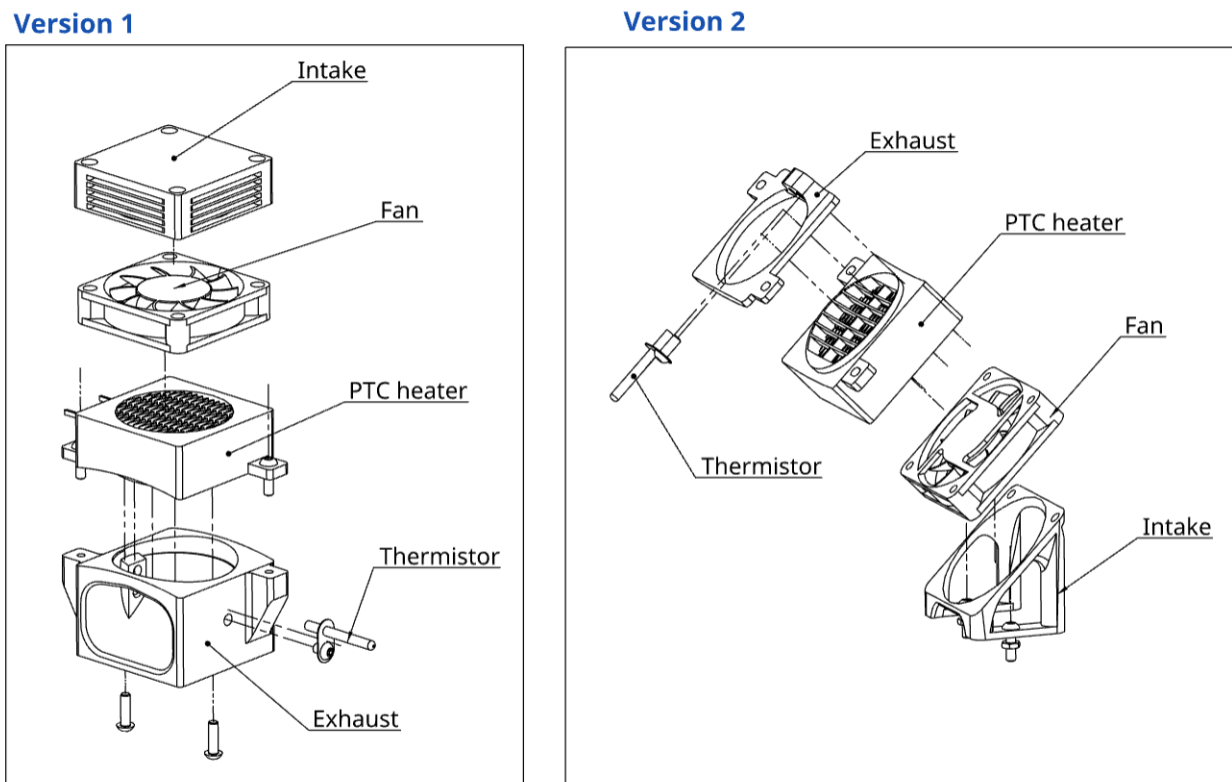


Figure 19: Heating unit versions

This revised design greatly improved the maximum temperature reached near the mold, as demonstrated later in Section 8.

## 5 Electrical design

### 5.1 Stepper driver

To control the stepper motors, the use of drivers is essential. For this project, the TMC2130 is an excellent choice. This driver is equipped with StealthChop Technology, which adjusts the current to prevent motor vibrations and noise.

The TMC2130 also features SPI communication, which makes it possible to receive full diagnostics of the motor and the driver. One of these features is stall detection which makes it possible to detect sensorless stalling, to stop the motors in the event of a stall and trigger an alarm signal.

However, only one feature can be used at a time, meaning a choice must be made between StealthChop and stall detection. In the event that rotation is obstructed, the motors will simply skip steps, which will not damage the machine itself. Since testing has shown a significant positive effect when StealthChop is enabled, this option is chosen to minimize ambient noise in the lab, as it could otherwise cause disturbance.

Furthermore, the controller is equipped with protection against overcurrent, overvoltage, and undervoltage.

In figure 20, the schematic of the driver is shown, along with how it is connected to the rest of the electronics.

To enable the motor, the enable pin has to be 0V. To make sure this pin is not floating, a pull down resistor is used as visible on Figure 21, causing the motors to start in the disabled state, unless otherwise specified by the microcontroller. The machine uses two stepper motors, and the configuration described above applies identically to both motors.

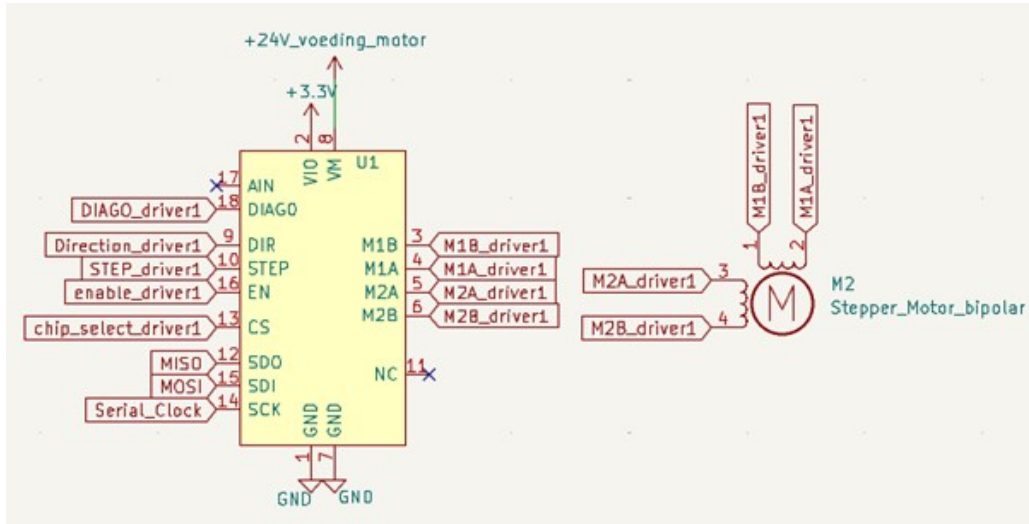


Figure 20: Stepper Motor Driver Schematic in KiCad

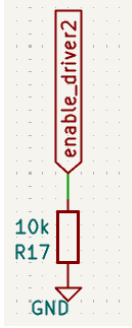


Figure 21: Enable Driver Schematic in KiCad

## 5.2 Heater

Raising the temperature accelerates the curing process of silicone. Therefore, incorporating a heating element can enhance the machine's throughput and reduce the duration of each prototype cycle. A PTC heater increases its resistance with increasing temperature, resulting in a power dissipation drop. This makes it a self regulating system which prevents extensive overheating. In figure 22, it can also be seen that this heater is controlled using a MOSFET, with a pull-down resistor of 10k ohm on the gate.

The heater will have a maximum power of 300W. At 24V, this results in a current of 12.5A. Since the resistance of the MOSFET between drain and source is 0.022 ohms at 3.3V, a power of 3.5W will be dissipated in the MOSFET. For this reason, a suitable heatsink has been chosen to attach to the MOSFET to ensure sufficient heat dissipation as well as a MOSFET with a sufficiently low on resistance. The IRLB3034PbF features an on resistance of max. 2.0 mΩ at a  $V_{GS}$  of 4,5V.

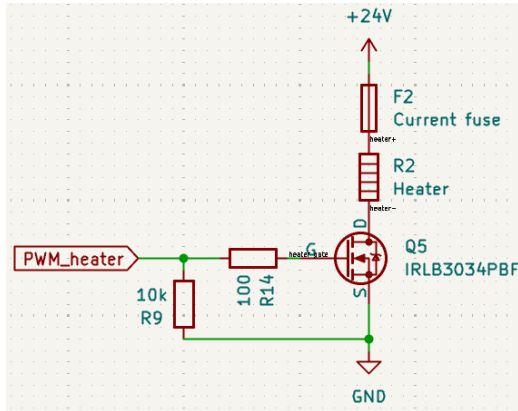


Figure 22: Heater and fuse in KiCad

## 5.3 Fans

In the entire design, three different external fans are used. The first one is used to blow the warm air, heated by the PTC heater, into the cabin. A MOSFET combined with a pull down resistor is used to control this fan. Additionally, two other fans provide a continuous airflow over the PCB to cool the electronics. These fans will start working after turning on the machine.

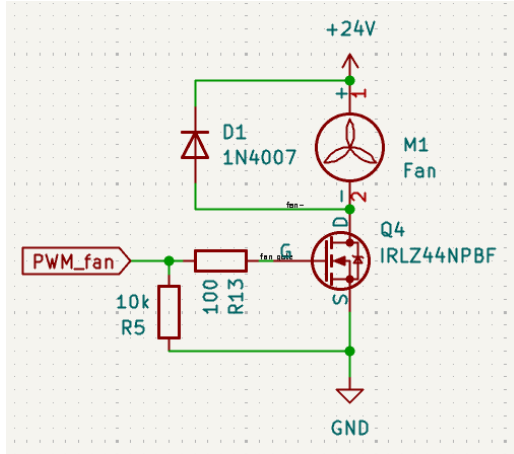


Figure 23: Fan next to heater Schematic in KiCad

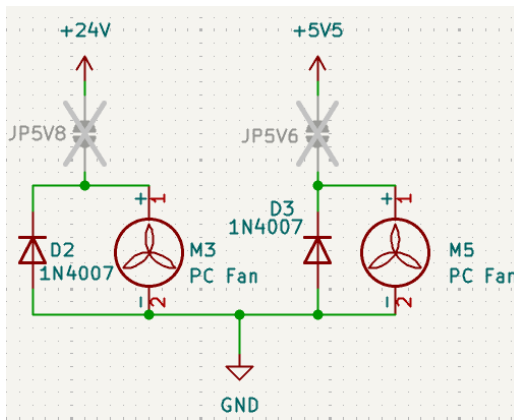


Figure 24: Fans to cool PCB Schematic in KiCad

### 5.3.1 Thermistor

To ensure that the temperature of the hot air blown into the enclosure always remains below a maximum limit, a temperature sensor is required. For this purpose, a thermistor is used. This sensor is placed directly in the hot air stream rather than elsewhere in the enclosure, as this prevents any local overheating that could potentially cause the plastic to melt. The KiCad implementation is visible in figure 25. Additionally, a 100-nanofarad decoupling capacitor is used to filter out noise. A 10k-ohm resistor is also used to complete the voltage divider of this measuring circuit.

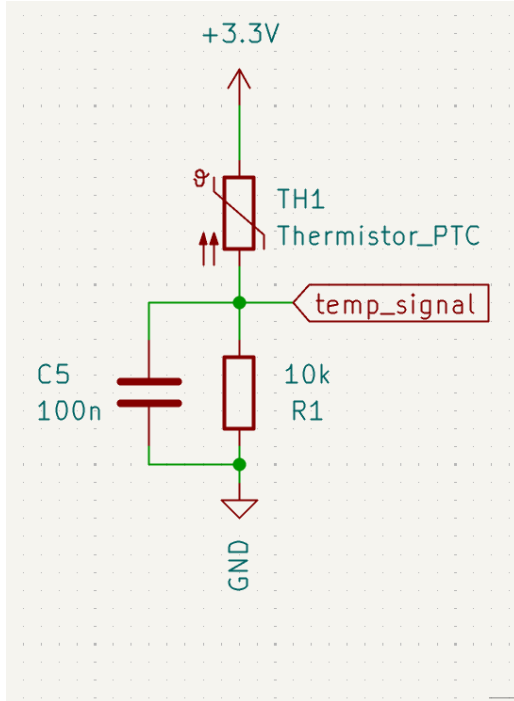


Figure 25: Thermistor in KiCad

## 5.4 Power

The various components operate at different voltages. Therefore, multiple conversions are required since the power outlet only supplies 220V AC. The power supply performs a conversion from 220V AC to 24V DC, as shown in Figure 26. A second conversion takes place on the PCB itself, using a 24V DC to 5V DC converter as shown in Figure 27. The final conversion is handled by the Pico itself, which converts the 5V DC to 3.3V DC.

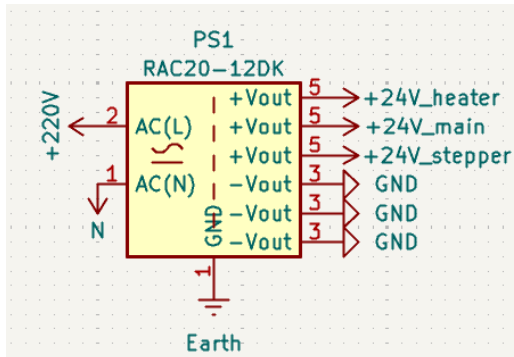


Figure 26: 24V Converter Schematic in KiCad

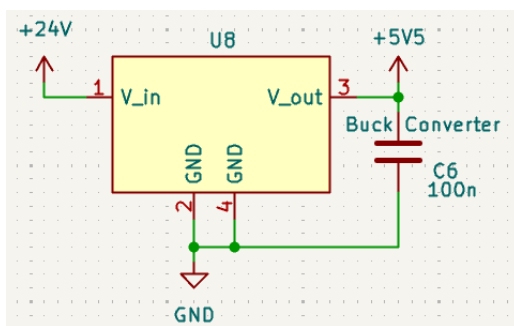


Figure 27: 5V Converter Schematic in KiCad

## 5.5 Microcontroller

The selection of the right microcontroller is based upon various requirements. In order to communicate with the various peripherals, 3 pins for the SPI protocol and 20 GPIO pins are needed. This makes the Arduino Nano (ATmega328p) unfit. Furthermore, good documentation of both the microcontroller and it's breakout board are required in order to have an effective electrical design. Plenty of ESP32 breakout boards don't feature this, hence, they are not suitable either. Lastly, the cost of the microcontroller should also be kept in mind to adhere as best as possible to the defined budget, which makes a microcontroller in the Teensy family unsuitable as well. Based on these requirements, a Raspberry Pi Pico is chosen with 26 GPIO, good documentation and low cost, whilst still having good performance with it's dual cores running a 32 bit architecture at 125MHz.

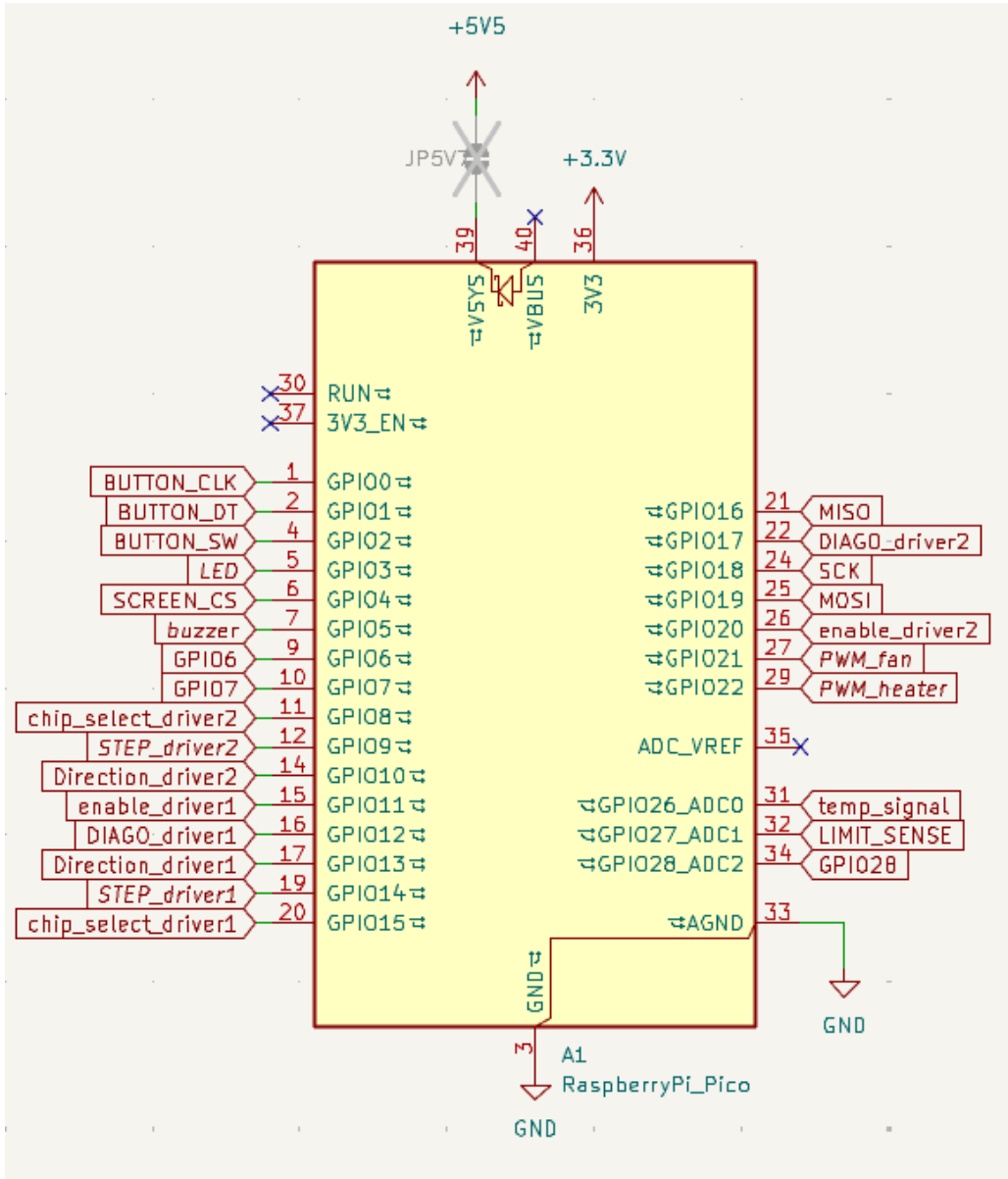


Figure 28: Raspberry PI Pico Schematic in KiCad

## 5.6 Fuse

To ensure safety, the machine is equipped with a current fuse that protects the PTC heater from short circuits. Figure 22 shows how this fuse is placed between the power source and the heater. Since the peak power of the PTC heater is 350 W and it is connected to a 24 V source, this results in a current of 14.6 A. The fuse has been selected with a nominal current rating of 20 A, and is therefore suitable for

this application.

The LED strip is also protected against overcurrent by a second current fuse, which safeguards against short circuits. The implementation of this fuse can be seen in figure 33.

Lastly, all the electrical components are protected by a 3A fuse on the main AC power lines. This provides more than the 600W that the power supply can supply, ensuring this fuse only burns when the PSU fails. It is located next to the main on-off switch of the machine.

## 5.7 E-stop

Another safety feature is the emergency stop (E-stop), which allows the machine to be shut down in case of an emergency. This E-stop is placed immediately after the power supply, so pressing it cuts off the entire power to the machine.

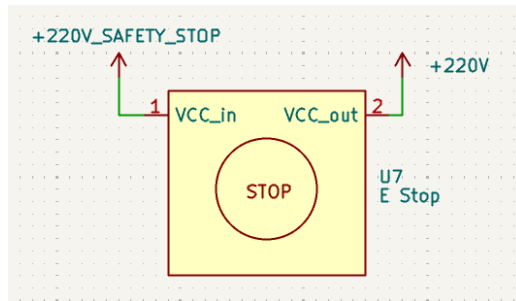


Figure 29: E-stop Schematic in KiCad

## 5.8 Limit switch

When the door is opened while the machine is running, it must immediately shut down to ensure safety. For this reason, a limit switch has been installed between the frame and the door. As shown in the KiCad schematic in Figure 30, the switch is connected to the normally closed (NC) pins. A high signal is therefore interpreted in the software as a closed door. Again, a decoupling capacitor is used to limit misreads and two resistors to complete the voltage divider. Additionally, opening the door can also trigger a signal to turn on the internal enclosure lighting, allowing for proper mounting of the mold.

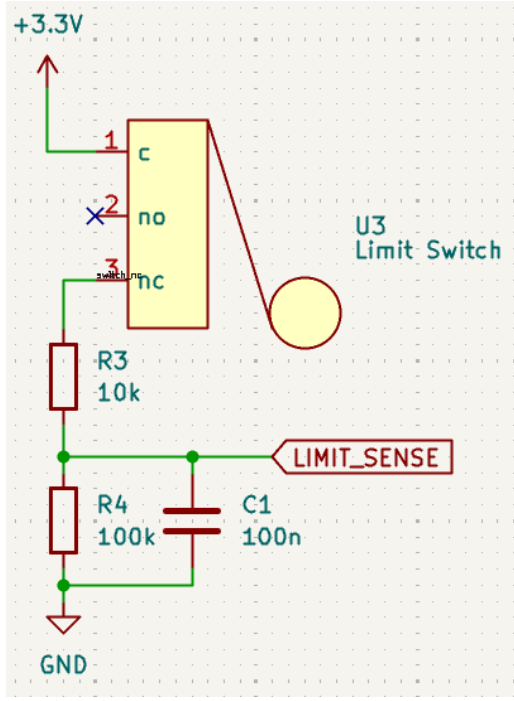


Figure 30: Limit switch Schematic in KiCad

## 5.9 Power socket

Using a power socket, the machine can be plugged into a wall outlet and switched on and off. The power socket itself is also additionally protected. Internally, it contains an extra fuse with a nominal current rating of 3 Amperes.

## 5.10 Display

Of course, the machine is clearly configurable. Program selection and addition are done via an LCD. The current progress of the program is also displayed on the LCD.

Increasing the amount of pixels improves readability but either increases the required bandwidth of the communication protocol or decreases the refresh rate of the display. Hence, a display of 128x64 pixels is chosen to provide a good trade off. The display should be connected as shown in Figure 31. Also, a 100 nanofarad capacitor is used as a decoupling capacitor.

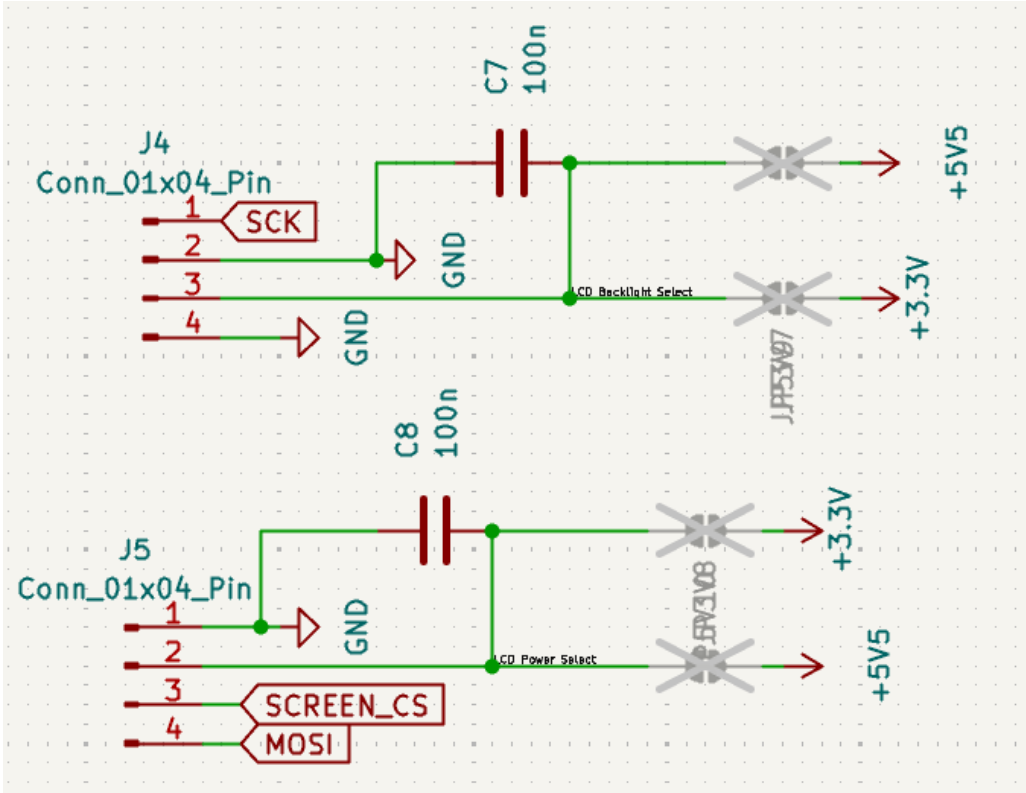


Figure 31: Screen Schematic in KiCad

### 5.11 Rotary push-button

To select the desired settings, the menu can be easily navigated using a rotary push-button, which allows for both rotational and push movements. To prevent floating, pull up resistors of 10k ohm are used. To prevent noise, the decoupling capacitors of 100nF are used on all output pins.

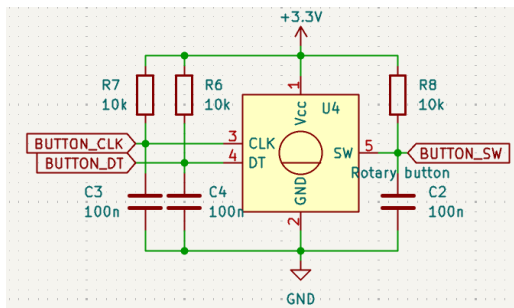


Figure 32: Rotary push-button Schematic in KiCad

### 5.12 LED-strip

On the inside of the frame, a long LED strip is mounted. This provides good lighting when attaching and detaching the mold. The LED strip is controlled using a MOSFET, with a pull-down resistor to ensure the gate pin is normally off and a gate resistor to limit gate inrush currents.

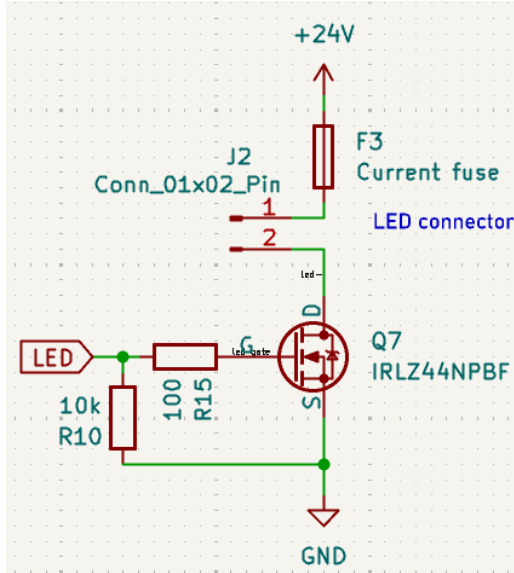


Figure 33: LED Schematic in KiCad

### 5.13 Buzzer

When the curing process is complete, the machine will emit an audible signal. This way, the operators present in the lab know that the mold is ready to be removed from the machine. A buzzer is used to produce this sound signal, as shown in Figure 34. To allow for different sound level options for the buzzer, the PCB was designed with three solder jumpers. For the final implementation, the buzzer was configured to operate at 5V. The buzzer is controlled using a MOSFET. In addition to the pull-down resistors at the MOSFET gate, a resistor was also placed between the two terminals of the buzzer to dissipate the stored energy from the buzzer.

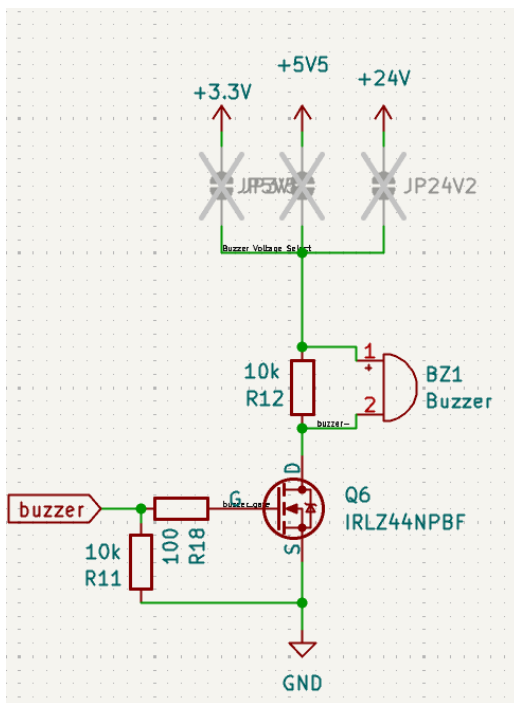


Figure 34: Buzzer Schematic in KiCad

### 5.13.1 Integration on PCB

To keep a clear overview of the pin configuration and their respective functions, table 5 can be used. Also Figure 28 gives a clear view of all the correct pins. Figure 35 provides a visualization of the PCB with all integrated components. Figure 36 shows the implementation of the PCB together with the wiring to all the peripherals.

GPIO	Name	Function	Extra
0	BUTTON_CLK	Rotary encoder B signal	
1	BUTTON_DT	Rotary encoder A signal	
2	BUTTON_SW	Rotary encoder push signal	
3	LED	LED strip line connected to the gate of a IRLZ44N MOSFET	
4	SCREEN_CS	CS line to address the LCD screen via SPI	Normally low
5	BUZZER	Buzzer line connected to the gate of a IRLZ44N MOSFET	
6	GPIO6	Extra GPIO pin	
7	GPIO7	Extra GPIO pin	
8	CS_DRIVER2	CS line to address the second driver via SPI	Normally low
9	STEP_DRIVER2	Step pin of driver 2	
10	DIR_DRIVER2	Direction pin of driver 2	
11	EN_DRIVER1	Enable pin of driver 1	
12	DIAG0_DRIVER1	Diagnostics interrupt pin of driver 1	
13	DIR_DRIVER1	Direction pin of driver 1	
14	STEP_DRIVER1	Step pin of driver 1	
15	CS_DRIVER1	CS line to address the first driver via SPI	Normally low
16	MISO	Master In - Slave Out line of SPI protocol for drivers and LCD	
17	DIAG0_DRIVER2	Diagnostics interrupt pin of driver 2	
18	SCK	Clock line of SPI protocol for drivers and LCD	
19	MOSI	Master Out - Slave In line of SPI protocol for drivers and LCD	
20	EN_DRIVER2	Enable pin of the second driver	
21	PWM_FAN	PTC fan line connected to the gate of a IRLZ44N MOSFET	
22	PWM_HEATER	PTC heater line connected to the gate of a IRL3705NPBF MOSFET	
26	TEMP_SIGNAL	ADC connected to the thermistor	
27	LIMIT_SENSE	ADC connected to the door limit switch	
28	GPIO28	Extra GPIO pin, can be used as ADC	

Table 5: GPIO Definitions

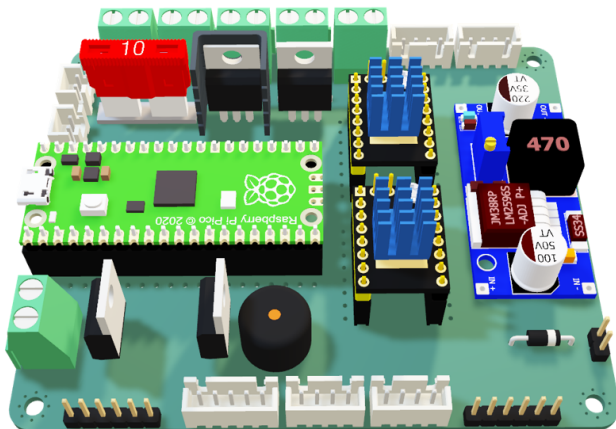


Figure 35: PCB integration on CAD model

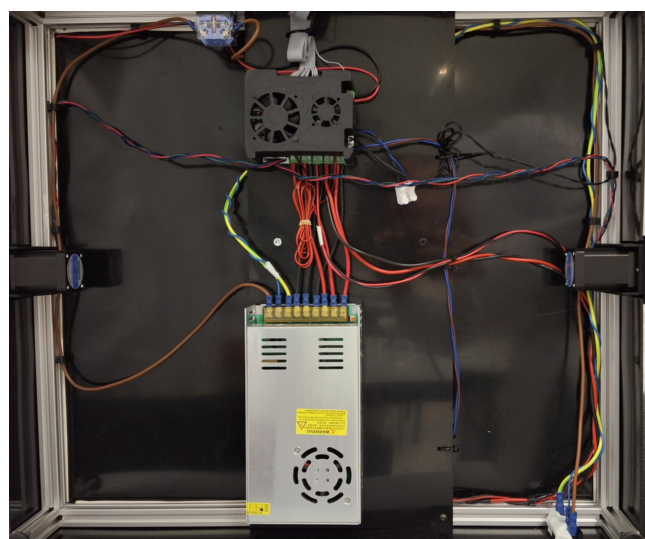


Figure 36: Electrical wiring

## 6 Software

In order to control the various mechanical and electrical components, software with multiple features has been implemented. These features include: gathering sensor information, storage and customization of various presets stored on local flash, user interface and menu navigation, driving and configuration of motors and heating and preheating of enclosure.

This is all implemented using the Arduino framework and the Arduino IDE, because of familiarity with the platform as well as to cut development time by using third party libraries.

### 6.1 Finite state machine

A Finite State Machine (FSM) is implemented to keep track of all the different states in which this machine can operate. The most important states are described in Table 6.

Name	Function
Home	Allow the user quick access to other states
Preheat	Preheat the enclosure
Quick start	Allow user to configure settings without needing to make a separate preset
Preset select	Allow user to store, edit, delete and add presets
Operation	Drive motors at desired speeds, do heater control and show status on screen

Table 6: Most important states in the FSM

In each of these states, three important tasks are executed. First, the processing of the rotary encoder is handled. Depending on the state, this sensor information is used to change variables or change states. Next, this information is used to update the display with the new data. Finally, depending on the state, other functions are executed. These include reading out the value of the thermistor, the control of the heater to achieve a desired temperature and the control of the stepper motors.

### 6.2 Sensor information

In order to make informed decisions about control, the machine is equipped with several sensors. These include a thermistor, a limit switch, a rotary encoder and motor drivers.

**Thermistor** The voltage between the  $10\text{k}\Omega$  thermistor and  $10\text{k}\Omega$  resistor is read out using one of the ADC pins and converted into a usable temperature reading using the Steinhart–Hart equation. The following library is used for this purpose: <https://github.com/panStamp/thermistor?tab=readme-ov-file>. Furthermore, an exponential averaging filter is used on this result to provide the user with a more slowly changing number.

**Limit switch** The pin connected to the limit switch is configured to a software interrupt which fires every time the switch changes states. In this interrupt, it checks the state of this pin, changes the variable that indicates the state of the door and decides whether or not to disable the steppers - which is crucial for safety - hence the interrupt based approach. It also triggers the LED strip to provide light to the user who has just opened the door.

**Rotary encoder** The state of one of the 2 encoder pins is checked continuously inside of the loop and compared to its state from the previous iteration. If this is different, the rotary encoder has moved. The state of the second pin is used to determine the direction of this movement. The rotary encoder also features an integrated push button. This is once again attached to an interrupt routine, which enables a flag to be processed inside of the main loop. A change in state of either the encoder or the

push button is registered and used to trigger both the LED strip and the display to refresh with the new information. To prevent double clicking/scrolling, a debouncing capacitor is used, as well as software debouncing.

**Motor drivers** The motor drivers are not only connected through STEP/DIR/EN lines to turn the motor, but also through the SCK/MOSI/MISO/CS lines. These are part of the SPI protocol and allow the Pico and TMC2130 driver to communicate with each other. This means the microcontroller can not only adjust settings such as max current or StealthChop (MOSI), but it can also receive information from the motor and driver like overtemperature warnings, estimated load level and stall detection (MISO). However, the TMC2130 drivers did not arrive in SPI mode out of the box. Desoldering of a  $0\Omega$  resistor on the bottom side of the driver, leaving the pad open, was needed to establish communication through SPI.

### 6.3 Flash

To keep the preset data stored in between power downs, they need to be stored in non-volatile memory. This can either be done using external components like an SD card or external flash, or by using the existing programmable memory already present on the Pico board. According to its datasheet, there exists a 2MB QSPI Flash used to program the Pico. However, there is no need to safeguard the full 2MB since the application only needs around 100 kB, or 5% of the space available on this flash.

In order to still keep a comfortable margin, user data is only written halfway on the flash, starting from address  $1024 \times 1024 = 1\,048\,576$ .

The user data is stored in one struct, starting with space for general settings, followed by the amount of presets present and the presets themselves.

The presets are also stored in a struct with 16 bytes for a name, followed by the settings themselves, stored as 32 bit signed integers resulting in a range of -2,147,483,648 ... 2,147,483,647. This range is more than sufficient for this application. 8 bit integers only provide a range of -127 ... 128 so as an improvement, the use of 16 bit signed integers can be used for this purpose.

Variable name	Data type	Function
Name	char	Store the name of the preset in 16 bytes
innerSpeedStart	int32_t	Speed of inner frame in dps at the start of operation
innerSpeedEnd	int32_t	Speed of inner frame in dps at the end of operation. Linear interpolation is used between start and end values.
outerSpeedStart	int32_t	Speed of outer frame in dps at the start of operation.
outerSpeedEnd	int32_t	Speed of outer frame in dps at the end of operation. Linear interpolation is used between start and end values.
durationHr	int32_t	Total hours of duration of operation.
durationMin	int32_t	Total minutes of duration of operation above the selected hour.
tempStart	int32_t	Temperature in °C at the start of operation.
tempEnd	int32_t	Temperature in °C at the end of operation. Linear interpolation is used between start and end values.

Table 7: Variables in each preset

The data on the user part of the flash is read out every time at startup and stored inside of volatile memory. If a preset is added, modified or deleted, this volatile memory is changed and overwritten onto the existing data of the flash.

## 6.4 User interface

One of the major tasks of the software is to provide a user interface to set and receive information from the user. The display consists of 128x64 pixels and is driven by the ST7920 driver using SPI. This driver is compatible with the U8g2 library which is used to provide some abstraction from the low level programming of this display. Some functions this library provides include the drawing of lines and boxes as well as the printing of text in various sizes and fonts. These functions are combined to provide a comprehensive user interface which fulfills all the requirements. By not having to implement these functions ourselves, this library reduced the development time of the project substantially.

The exact library used for the application can be found in the documentation, see Section A.

The machine boots up and shows the home screen. From this screen, the user can select a preheat function, a quick start function, a list of presets and general sensor information. On the preset screen, the user sees a list with all of the presets that previously have been made, as well as the option to add a new preset and a standard '*Last used*' preset, which stores the settings from the last operation. When a preset is selected or added, the user can edit the preset and its name as well as delete it or use it for operation.

When in operation, the user is presented with key information such as inner and outer frame rotational speeds, as well as the temperature readings from the thermistor and the remaining time.

The user can also select one of the motors, the heater or the preset info widget to gain more information about the selected feature. In order to provide the user with more information about the current state of these peripherals.

## 6.5 LED strip

The LED-strip is controlled by the microcontroller using a MOSFET. This allows the LED strip to be turned off to save power when in idle operation and allows for the adjustment of its brightness.

When a user input is registered in the form of a rotary encoder input, limit switch change in state or the door that is open, dedicated software is triggered. This software provides a soft rampup in duty cycle of the PWM pin and thus in light intensity over 1s when a first input is detected and keeps the light on for one minute if no subsequent user inputs are received. If no user inputs have been detected over this time period, the code provides a soft rampdown in PWM duty cycle to shut off the lights in a smooth way.

To enable these functions, a custom library has been written and can be found in the documentation, see Section A.

## 6.6 Stepper motor control

In order to communicate with the driver's chip and to configure settings like maximum motor current or StealthChop, the driver is adjusted into SPI mode by desoldering a  $0\Omega$  resistor and connected through the SPI lines: SCK, MOSI, MISO and CS.

The TMC2130 stepper library is used to provide us with the low level register reading and writing functions, as well as more high level functions like the enabling of StealthChop or StallGuard or the adjustment of microsteps.

The exact library used for the application can be found in the documentation, see A.

In order to allow the motors to rotate, the motor drivers require a STEP, EN and DIR signal. The STEP signal tells the driver to advance the magnetic field of the stator with one step. Depending on the configuration of microstepping, this results in a rotor angular displacement of anywhere between  $1.8^\circ$  and  $25''$ .

The EN pin tells the driver whether or not to enable the motor. Pulling this pin low enables it, sending current through the motor coils and trying to keep the stepper at its current orientation. Pulling this pin high disables the steppers, allowing them to move freely without consuming current.

Lastly, the DIR pin tells the driver in which direction the motor should rotate and allows it to adapt the currents sent to the motor coils accordingly.

To get a constant speed from these stepper motors, requires a constant frequency of switching on the STEP pin of the motor driver. There are many approaches to drive these pins, such as bit-banging with delays, using the second core of the Pico, using direct hardware PWM to the pins, or using hardware PWM to trigger internal interrupts. Many of these techniques have been tested and implemented but nothing was as reliable as setting a fixed interrupt frequency of 100kHz to poll the state of both step pins and switch them based on the time that has passed after the previous switch. By varying this time, which is effectively half the period of our signal, the frequency of the step signal and thus the rotational speed of the two motors can be controlled.

## 6.7 Heater control

To control the heater, a PID controller is implemented, with input signal the error between the reference temperature and the thermistor readings and as output signal a binary decision to turn the heater on or off. The controller calculates an output between 0 and 1 every 100ms. If this output falls below 0.5, the heater turns fully off for this time period, if the PID output is calculated to be above 0.5, the heater turns on.

When designing the PCB, the output signal was expected to be the duty cycle of a fast switching PWM signal. However, when implemented, this fast switching of these high currents caused a high pitched noise. Hence, the former control method is preferred with similar performance due to the high time constants in thermal systems.

These calculations are only made when the user has selected the preheat option or if the state machine is inside operation and a target setpoint of more than 20 degrees C has been set.

The cold air is pushed through the heating unit using a fan. This fan turns on if either the **heater** is turned on and control calculations are being executed or after the heater is turned off but the **temperature** of the heating element and the air that passes through it is above 25 degrees C.

## 7 Budget

All aspects of the design and component selection were executed with a target budget of € 500, which is quite limited to accomplish all these features. During component selection, it became apparent that the budget requirement was not feasible given the functional requirements. In consultation with the commissioning supervisors, it was decided to prioritize retaining the functional requirements over strictly adhering to this target budget.

The final budget spent was € 611.73 (excl. VAT), a more detailed breakdown is shown in Table 8. This is over budget, but still cheaper than a rotocasting machine with similar mold capacity on the market [2] costing \$1,200.00 USD. Note that this example does not feature an enclosure or heating, but on the other hand cost of labor is not included in our budget which would be more expensive than the components shown.

<b>Electrical</b>		
	Interface	€ 24.42
	Safety switches/stops	€ 20.79
	PCB	€ 12.86
	Heater	€ 10.34
	Cooling	€ 8.69
	Sensors	€ 3.83
	Drivers	€ 27.65
	Stepper motors	€ 14.17
	Micro controller	€ 3.67
	Power supply	€ 41.34
	LED lighting	€ 3.09
	Connectors	€ 16.25
	<b>Subtotal</b>	<b>€ 187.10</b>
<b>Mechanical</b>		
	Frame extrusions	€ 58.93
	Axles	€ 11.20
	Bearings	€ 23.34
	Belts	€ 20.87
	Pulleys	€ 34.77
	Fasteners	€ 68.03
	U channel	€ 5.93
	Latches, catches and handles	€ 27.97
	Polycarbonate plate	€ 39.82
	HDPE plate	€ 55.09
	3D printing materials	€ 53.29
	Miscellaneous	€ 25.40
	<b>Subtotal</b>	<b>€ 424.63</b>
<b>Total</b>		<b>€ 611.73</b>

Table 8: Budget overview

## 8 Testing

Some initial rotational casting test were conducted with the assembled machine to assess its functionality and find potential issues. First an overview is given of the conducted test and the achieved results. Subsequently the performance of the machine in the test is discussed, highlighting what works as intended and where there is room for improvement.

All implemented safety features such as emergency stop, door sensor and enclosure work as expected and ensure safe operation.

### 8.1 Overview of test

For the initial test, a mold of a light bulb was designed and 3D printed shown in Figure 37. This combines a simple, spherical feature with some more complex and fine features such as threads. The testing approach used is exploratory, meaning process parameters and silicone were selected that seemed like they could provide some interesting or insightful results.

The silicone mass used (50 g) was intended to produce a wall thickness of 3 mm. The silicone was properly mixed, and all air bubbles were removed using a centrifuge and finally poured into the mold. The mold walls were treated with mold-release to make removal easier. The curing process was accelerated by using the machine's built-in heating system.

In the first test, the mold was rotated at a speed of 4 RPM on the outer axis and 1 RPM on the inner axis. This resulted in a light bulb where the silicone was not evenly distributed throughout the mold. The entire shape was not airtight.

To continue testing, the same test was repeated, but this time with thinner added at a ratio of 8 % relative to the amount of silicone used. This made the silicone less viscous, allowing it to spread more easily throughout the mold interior. Although the silicone was still not perfectly evenly distributed in this second test, the results were significantly better than the first. Moreover, this time the mold was airtight and the final shape was solid. This was the best result obtained in the limited tests conducted.

For the third test, a silicone with a lower Shore hardness was used, as it was less viscous and the previous test suggested less viscous (thinned) silicone performed better. The rotation speeds were reduced to allow the silicone more time to flow. This did not have the intended effect, as the issue of uneven silicone distribution became even more pronounced. A large clump of silicone formed in the center of the light bulb.

In the final test, the first silicone was used again, this time with 10 % thinner by weight. The machine was also operated at even lower speeds. This again produced no improvements, as the silicone was once again distributed very unevenly throughout the mold.

An overview of the used settings is provided in Table 9, and the results of all tests are shown in Figure 37 where the results are sorted in order of test number from left to right. A more detailed view of the best result is shown in Figure 38.

Based on these tests, it is clear that the machine is capable of performing its intended function. However, the optimal operating parameters still need further research, due to the current lack of knowledge regarding an ideal curing process in a rotational casting machine. This includes more methodological testing and/or modeling the process. This is however out of the scope of this project.



Figure 37: Experimental mold and results



Figure 38: Second test - silicone light bulb

Test nr.	Silicone Shore A hardness	wt% thinner	Outer rpm	Inner rpm
1	50	0	4	1
2	50	8	4	1
3	5	10	1.33	0.33
4	50	10	0.67	0.17

Table 9: Test parameters

## 8.2 Machine performance

In general, the machine is fully functional and its core features work properly. The interface, navigation, mold mounting and balancing are all relatively fast and easy to use. The only tedious part is fastening the mold to the plate as expected, but with some improvement to mold design this could be simplified.

### 8.2.1 Mechanical

The frame is strong and stiff, as predicted by the design calculations, whilst still being light. The kinematics work well, the frames can rotate smoothly without noticeable radial play. The belt transmission system is fully functional; the belts do not skip, can be tensioned sufficiently and run smoothly.

A small improvement could be the use of belts with larger teeth that are slightly more robust and optimizing belt paths to be as straight as possible.

The selected motors proved powerful enough in testing, and can easily accelerate the frames up to speeds when loaded. As a 5 kg weight was not available the maximum capability could not be tested, but there were no indications this load would be too much. Testing also revealed that the ability of the stepper motors to maintain very low speeds ( 0.5 rpm) smoothly is very useful. This would be much harder for BLDC motors, confirming the decision to use stepper motors was a good one.

The mounting system proved effective, relatively easy to use and fast. The plate is strong and can be mounted very securely, whilst also being easy to insert and remove. The transparent polycarbonate allows easy inspection of the process and makes fastening molds easier as tools under the plate can be seen while manipulating the mold on top of the plate. The adjustable handles are effective and allow easy and fast balancing of the mold in the machine. The toolless latching and adjustments are functional and user friendly.

There is of course some room for improvements. The latches can be tightened with one hand, but it is not that easy to do so as they are small and really powerful. A possible remedy for this would be to use slightly larger latches, but as these were not found they would likely need to be custom made which is expensive. It is also a little inconvenient that the sliding brackets on either side of the plate are not synchronized and can thus easily be misaligned. This is not a big issue, as it only requires some extra attention while adjusting.

The heating system falls far short of expectations. As discussed earlier, the fan inside the heater is simply not powerful enough to transfer the heat from the PTC element to the enclosure air. The heater could not be turned on at full power by the PID controller as it would overheat without increasing enclosure temperature significantly.

To illustrate this, and also to compare the two heater unit iterations a heat-up test was performed. The setpoint of the heater was set as high as possible. The maximum setpoint was 60°C for the first heating unit version as the exhaust was close to the HDPE panels. For the second version this maximum could be increased to 80 °C, as the exhaust did not blow directly on or past a panel at a small distance. The temperature around the plate was measured using a simple battery operated thermometer. The results of this test for both iterations is shown in Figure 39, along with the simulated one.

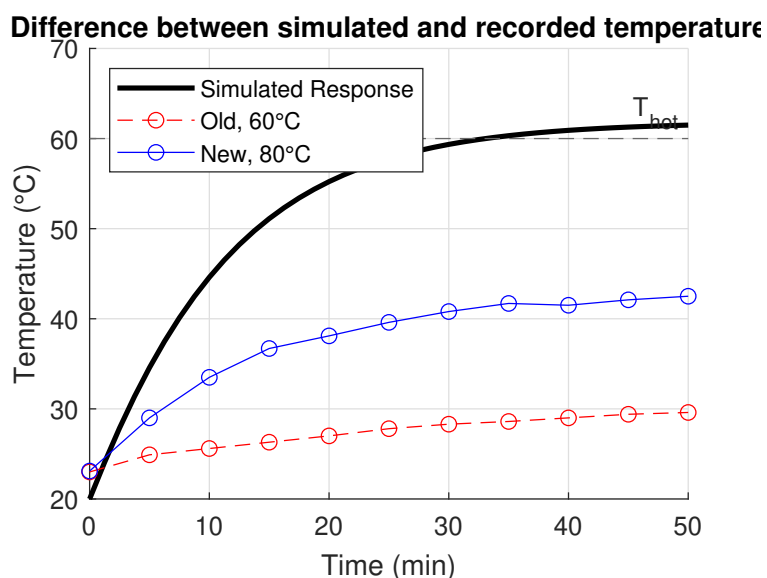


Figure 39: Enclosure heating test results

The achieved temperature increase, especially with the second heating unit version, is significant enough to make a large difference in curing time. But it still falls short of the set goal.

Besides the heater, this could also be improved by adding some insulation to the enclosure panels. The current enclosure is strong enough to protect the user, but still lacks some stiffness and insulation. The panels deform too much due to mounting bolt pressure and gravity, indicating a thicker plate or different material would be better. There is also plenty of room inside to mount insulation inside the panels, making the machine more efficient. Both of these measures would significantly increase the cost of the machine.

### 8.2.2 Electronics

In general, all electronics performs as intended, and no major issues were found during testing. There are a couple minor points that could be improved, but the machine is fully functional.

- The selected stepper motor driver can not do stall detection and silent operation simultaneously. While not a large problem as outlined earlier, a driver capable of both would no doubt be an improvement.
- These stepper drivers are also prone to overheating due to an outdated design using transistors with relatively high on resistances. Even with big heat sinks and forced airflow of the electronics fan, these drivers are limited to delivering 600mA. This is still sufficient to provide the torque for the requirements, but is undersized for the selected motors. In this way the machine functions with no issues, but the root cause behind this was not found nor is it certain whether this is a software configuration problem or electrical design flaw.
- In the current implementation, the fans that cool the PCB cannot be turned on or off. Even when the machine is not operating but simply powered on, these fans will still make noise, which can be perceived as disturbing. Using a MOSFET can solve this issue. Our microcontroller still has several available pins, so there is room to control these two MOSFETs.
- Another improvement could involve choosing different terminal blocks. The cables, which were selected based on the current they need to carry, are slightly too thick to fit easily into the current terminals.
- In the PCB design, the limit switch was not correctly connected to ground, which caused it to not function initially. This was easily fixed by soldering an external wire to the PCB.
- During the development and testing phase of the machine, the PCB was continuously connected to a computer. At that stage, the Raspberry Pi Pico was powered via the USB connection through the VBUS pin. Later, when the machine is expected to operate autonomously, a 5V supply from the machine's power source is used, connected to the VSYS pin.

To switch between these two power sources, a solder jumper was integrated into the PCB design, allowing for a simple manual connection. However, the placement of this jumper is unfortunate—as shown in Figure 40—since it is located among other densely packed components, making it difficult to access and solder. A recommended improvement would be to reposition this jumper closer to the edge of the PCB for easier access during modification.

An intermediate solution is provided by breaking out these pads outside of the electronics enclosure and bridging the gap with a push type wire connector for easy access, as shown in Figure 41. When uploading new code and plugging in a separate 5V signal through the USB port, it is recommended to disconnect this to separate the PCB power supply from the USB power, preventing damage to the device used to upload code.

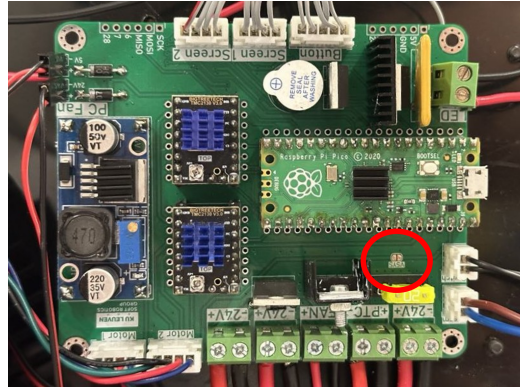


Figure 40: PCB integration with jumper marking

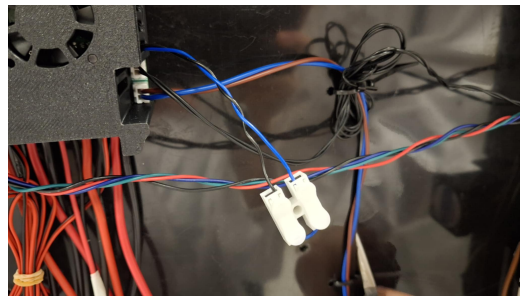


Figure 41: Extension of the solder jumper

### 8.2.3 Software

The software is fully functional, and provides quite intuitive and extensive control over the machine. It has some small issues, in some menus the incremental encoder used to scroll sometimes skips a step. This is not really an issue, the navigation still remains responsive.

To further improve on software, new functionalities can be added. During testing, it became clear that allowing the silicone to cure slowly at the beginning when it is still inviscid, and letting it cure faster after this time would be a useful feature. This could be realized by adding a heating delay before which the heater remains turned off to allow for longer and better distribution of the silicone.

## 9 Conclusion

The designed, constructed and tested machine meets nearly all requirements that could be tested, apart from the target budget. The optional heating requirement was implemented, but its design leaves a lot of room for improvements, mainly in heater fan power and enclosure insulation.

Further testing will reveal if the heating is sufficient and if it even is beneficial or increases silicone viscosity too fast.

The mechanical frame, kinematics and transmission perform as intended, supported by a fully functional electrical system that also performs as desired. The software provides intuitive and extensive control over currently controllable process parameters. Testing will reveal if the level of control is sufficient or if additional settings are required.

The machine is user friendly with clear illumination, toolless operation and adjustments that are intuitive and fast to use. The machine operates at a noise level that does not disturb other lab users, and has the necessary safety features to not pose a risk to its environment and users.

All this together makes this machine a good starting point for research into fabrication of soft robots through rotational casting. It provides a solid and functional basis to start developing molds and process parameters that expand the current possibilities in soft actuators. This testing should find the limitations of the current machine, and if necessary improvements can be made in future iterations along with the improvements suggested in this report. In the event the current machine proves insufficient, implementing these incremental improvements discussed above should turn this proof-of-concept machine into a dependable lab tool that consistently produces uniform, seam-free soft actuators in a single step.

## References

- [1] Mannetron. 2' x 2' rotational casting machines — mannetron.
- [2] HackMakeMod. Rotocast digital, n.d. Accessed: April 3, 2025.
- [3] Dan Maloney. A rotocasting machine sized for the home shop — hackaday.
- [4] Stelter Creative. Rotational casting — tilted tombstone.
- [5] Te Faye Yap, Anoop Rajappan, Marquise D. Bell, Rawand M. Rasheed, Colter J. Decker, and Daniel J. Preston. Thermally accelerated curing of platinum-catalyzed elastomers. *Cell Reports Physical Science*, 5:101849, 3 2024.
- [6] J.R. Culham, M.M. Yovanovich, and S. Lee. Thermal modeling of isothermal cuboids and rectangular heat sinks cooled by natural convection. *IEEE Transactions on Components, Packaging, and Manufacturing Technology: Part A*, 18(3):559–566, 1995.

## A Machine documentation

<https://github.com/JarneVG/RotocasterKUL.git>

### A.1 Quickstart guide

The machine boots up and shows the home screen. From this screen, the user can select a preheat function, a quick start function, a list of presets and general sensor information. On the preset screen, the user sees a list with all of the presets that previously have been made, as well as the option to add a new preset and a standard '*Last used*' preset, which stores the settings from the last operation. When a preset is selected or added, the user can edit the preset and its name as well as delete it or use it for operation.

When in operation, the user is presented with key information such as inner and outer frame rotational speeds, as well as the temperature readings from the thermistor and the remaining time.

The user can also select one of the motors, the heater or the preset info widget to gain more information about the selected feature. In order to provide the user with more information about the current state of these peripherals.

#### A.1.1 Loading mold

To load a new mold the perforated plate first need to be removed from the machine so it is easier to mount the mold to the plate. This can be done by loosening the two latches shown in figure 42. After this the plate is able to freely slide out of the C-channels.

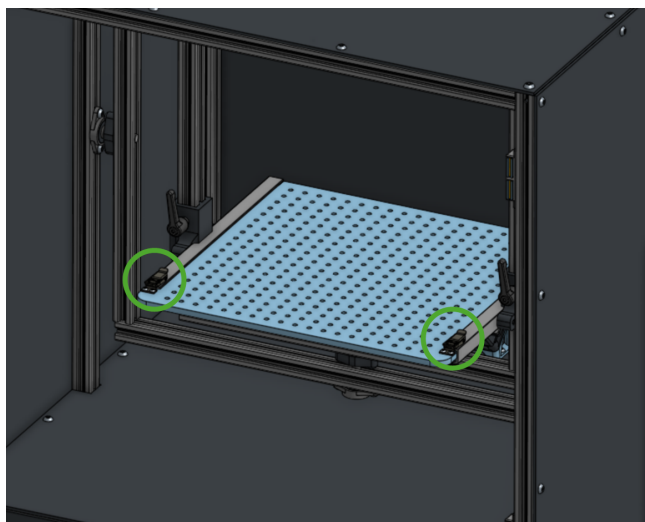


Figure 42: Latches of the plate system

The mold needs to be designed with the mounting holes for the plate system in mind. The holes on the plate are spaced out in a grid 15 mm apart from one and other. The holes have a diameter of 4.5 mm and will fit M3/M4 bolts. The mold can be mounted to the plate system by inserting threaded rods or bolts trough the mold and securing them with washers and nuts to the plate.

Before placing the plate with mold back into the machine it is important to check that the mold is placed in the center of the plate so it is balanced. After sliding the plate into the C-channels and making sure both latches are secured the machine can be further balanced in order to minimize vibrations. This is done by firstly moving the entire plate assembly up and down using the two handles attaching it to the frame and secondly by moving the two smaller weights attached to the bottom and top of the inner rotating frame.

Figure 43 shows the location of the balancing weights and the handles to move the plate assembly up and down. Always make sure the handles are aligned with the inner frame vertical extrusions to prevent collisions.

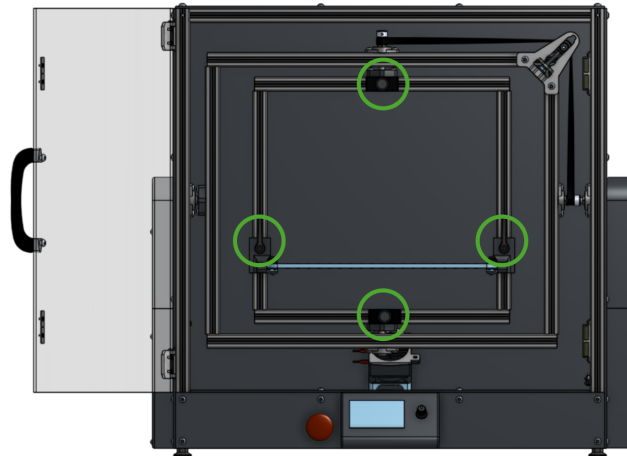


Figure 43: Balancing weights

## A.2 Maintenance

Belt tension should be checked at regular intervals ( 3 months) or when the machine does not operate as expected. When the frames have a lot of slack when the motors are engaged or when load rattling sounds/vibrations are heard from the motors/pulleys, the belt tension should be checked.

When the belt is too loose, it will experience excessive wear due to (teeth) slipping. When the belts are too tight, the bearings of the motors and frames will wear faster. As a rule of thumb, when the belt is tight enough to make a low pitched but distinct note when plucked like a string, the belt tension is sufficient.

To change belt tension on the inner belt, tighten/loosen the tension adjustment nuts as shown in Figure 44 on either side simultaneously and check belt tension by plucking the belt like a string until the tension is sufficient.

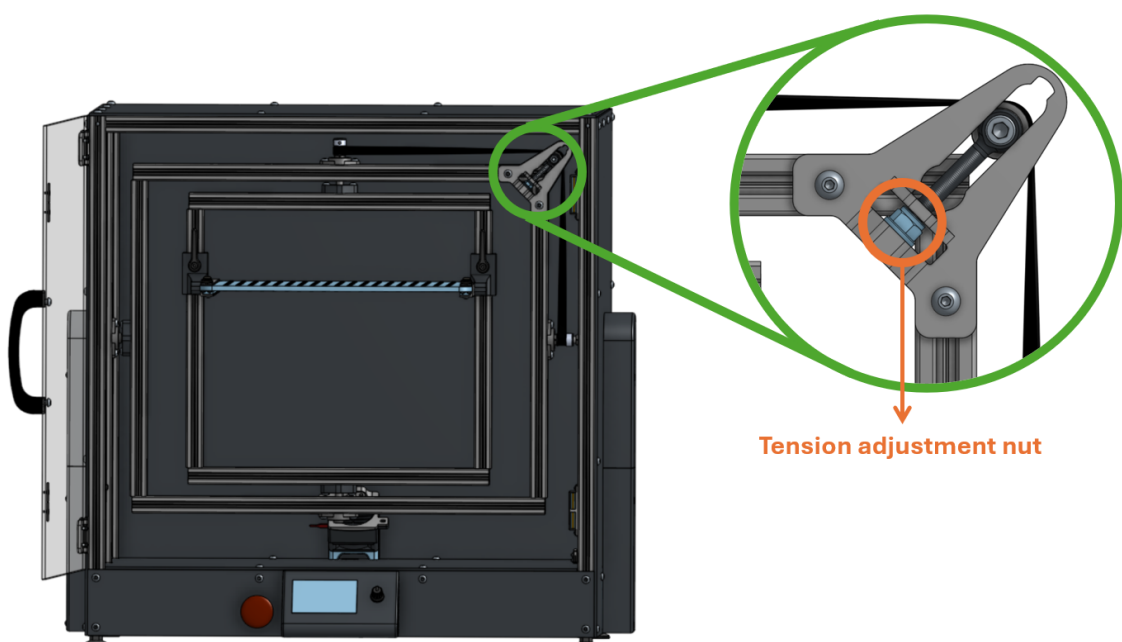


Figure 44: Inner belt tension adjustment

To change the tension of the belts on the side, first remove the lower and upper belt cover in that order by undoing the three M4 screws highlighted in Figure 45 holding them onto the machine.

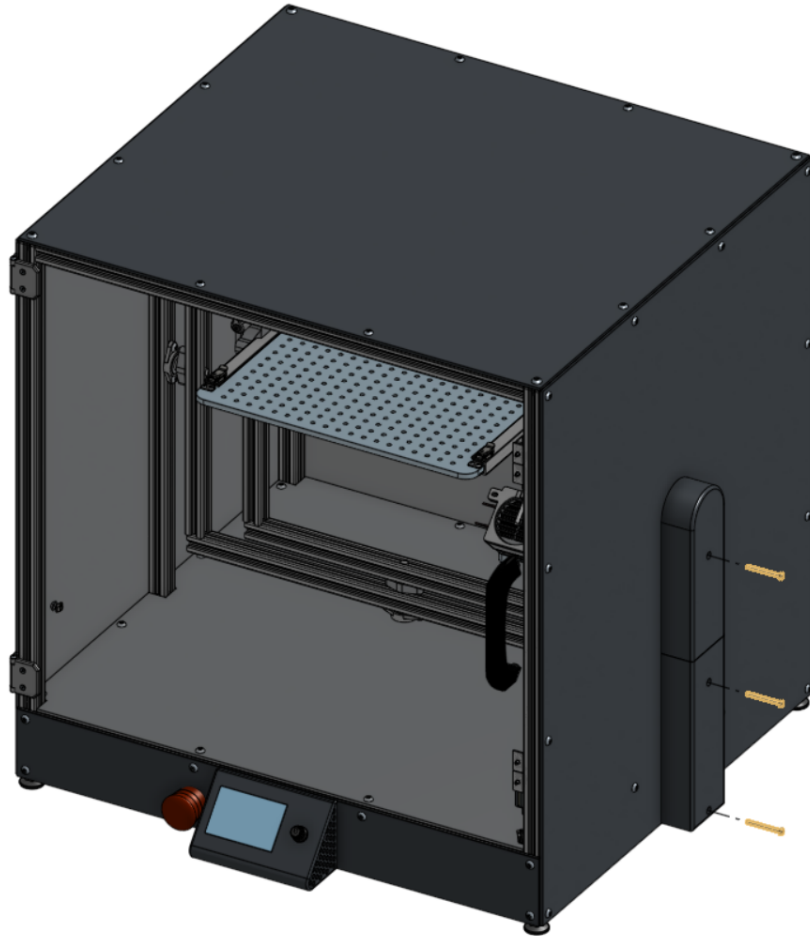


Figure 45: Belt cover screws

The belt tension can be adjusted by changing the motor position by loosening the four M3 screws highlighted in Figure 46.

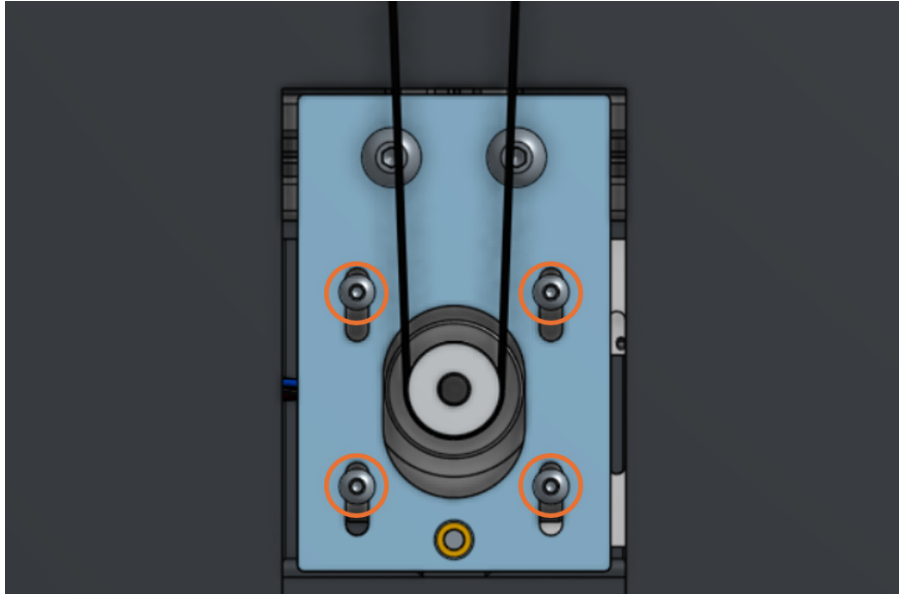


Figure 46: Motor mount screws

The procedure is the same on either side, but note the right belt covers are slightly larger.

### A.3 Flashing new software

If changes need to be made to the source code, there need to be several adjustments on your computer in order to do so.

First, be sure to disconnect the Pico from the 5V internal power supply in order to prevent current flowing into your laptop through the 5V your USB cable provides. You can reconnect the Pico to the 5V rail once we are done with uploading and when you have disconnected your laptop. See section 8.2.2 for more details.

Next, since we are using a Raspberry Pi Pico, which is not a standard Arduino but can be programmed with the Arduino framework, we need to install the Earle Philhower core.

This involves pasting the following under Additional Board Manager URLs from File → Preferences:

```
https://github.com/earlephilhower/arduino-pico/releases/download/global/package\_rp2040\_index.json
```

And subsequently installing the Raspberry Pi Pico/RP2040 boards from the Tools → Board → Board Manager.

A more detailed explanation can be found here:

<https://learn.adafruit.com/rp2040-arduino-with-the-earlephilhower-core/installing-the-earlephilhower-core>

Sometimes however, it is needed to press the BOOTSEL button on the Pico while powering it on to force it into boot mode. This is usually not necessary, but know that this sometimes can happen. When uploading fails, the final message of the compiler will be: 'No drive to deploy'.

A good guide on how to flash the firmware on the pico can be found here:

<https://randomnerdtutorials.com/programming-raspberry-pi-pico-w-arduino-ide/>

### A.4 Documentation of software

The source code and the actual libraries that were used for this project can be found on Github:

<https://github.com/JarneVG/RotocasterKUL.git>

The code is organised into several .ino files based on state or functionality. When opening either one of these files in the same folder, the Arduino IDE opens all of them and sorts them as tabs. For example, you can find the separate stepper functions inside the Steppers.ino file and the functions running when in the operation state in the Operation.ino file.

## B Logbook

**Week 1 Dates:** Feb 10 – Feb 14, 2025

Member	Actions
Jonas Thewis	Gathering information, defining requirements and drafting Gantt chart
Jarne Van Geyseghem	Gathering information, defining requirements and drafting Gantt chart
Rik Vanhees	Gathering information, defining requirements and drafting Gantt chart
Renaat Van Wayenberge	Gathering information, defining requirements and drafting Gantt chart

**Week 2 Dates:** Feb 17 – Feb 21, 2025

Member	Actions
Jonas Thewis	Gathering information, defining requirements and working on conceptual design
Jarne Van Geyseghem	Gathering information, defining requirements and working on conceptual design
Rik Vanhees	Gathering information, defining requirements and working on conceptual design
Renaat Van Wayenberge	Gathering information, defining requirements and working on conceptual design

**Week 3 Dates:** Feb 24 – Feb 28, 2025

Member	Actions
Jonas Thewis	Focussing on electrical design
Jarne Van Geyseghem	Focussing on electrical design
Rik Vanhees	Focussing on conceptual mechanical design
Renaat Van Wayenberge	Focussing on conceptual mechanical design

**Week 4 Dates:** Mar 3 – Mar 7, 2025

Member	Actions
Jonas Thewis	Sourcing of electronics
Jarne Van Geyseghem	Sourcing of electronics
Rik Vanhees	Designing frame
Renaat Van Wayenberge	Working on mechanical design and sourcing of parts

**Week 5 Dates:** Mar 10 – Mar 14, 2025

Member	Actions
Jonas Thewis	Sourcing of electronics
Jarne Van Geyseghem	Sourcing of electronics and start of interface software
Rik Vanhees	Designing transmission and rotating components
Renaat Van Wayenberge	Working on mechanical design and sourcing of parts

**Week 6 Dates:** Mar 17 – Mar 21, 2025

Member	Actions
Jonas Thewis	Sourcing of electronics and KiCad implementation
Jarne Van Geyseghem	Further interface software (miniature OLED screen and encoder)
Rik Vanhees	Designing enclosure

Renaat Van Wayenberge	Working on mechanical design and sourcing of parts
-----------------------	----------------------------------------------------

**Week 7 Dates:** Mar 24 – Mar 28, 2025

Member	Actions
Jonas Thewis	KiCad implementation
Jarne Van Geyseghem	Interface software: finite state machine logic + smooth LED code
Rik Vanhees	Finalizing mechanical design and the bill of material
Renaat Van Wayenberge	Working on mechanical design, sourcing of parts and presentation

**Week 8 Dates:** Mar 31 – Apr 4, 2025

Member	Actions
Jonas Thewis	KiCad implementation
Jarne Van Geyseghem	Interface software: finite state machine displays, finalization and ordering of PCB & KiCAD
Rik Vanhees	Finalizing mechanical design and presentation
Renaat Van Wayenberge	Finalizing mechanical design and presentation

**Week 11 Dates:** Apr 21 – Apr 25, 2025

Member	Actions
Jonas Thewis	Electronics assembling
Jarne Van Geyseghem	RP2040 Flash coding, PCB soldering
Rik Vanhees	Assembling frame
Renaat Van Wayenberge	Fabrication of (3D printed) components and starting assembly

**Week 12 Dates:** Apr 28 – May 2, 2025

Member	Actions
Jonas Thewis	Electronics assembling and assembling electronics on the machine
Jarne Van Geyseghem	Testing motor software + SPI + StealthChop + current limit
Rik Vanhees	Assembly of the rotating frames and transmission
Renaat Van Wayenberge	Fabrication of (3D printed) components and assembly

**Week 13 Dates:** May 5 – May 9, 2025

Member	Actions
Jonas Thewis	Assembling electronics on the machine
Jarne Van Geyseghem	Integration of software and electronics + lots of debugging
Rik Vanhees	Assembly of the enclosure
Renaat Van Wayenberge	Fabrication of (3D printed) components, finalizing assembly and redesign

**Week 14 Dates:** May 12 – May 16, 2025

Member	Actions
Jonas Thewis	Cable management and writing report
Jarne Van Geyseghem	Lots of debugging code + writing report
Rik Vanhees	Fixing last issues and testing the design

Renaat Van Wayenberge	Fabrication of (3D printed) components, testing and integration, writing report
-----------------------	---------------------------------------------------------------------------------

**Week 15 Dates:** May 19 – May 23, 2025

Member	Actions
Jonas Thewis	Writing report
Jarne Van Geyseghem	Debugging + Writing report
Rik Vanhees	Testing and writing report and presentation
Renaat Van Wayenberge	Testing and writing report and presentation

## C Gantt chart

Task description	Week 1	Week 2	Week 3	Week 4	Week 5	Week 6	Week 7	Week 8	Week 9	Week 10	Week 11	Week 12	Week 13	Week 14	Week 15
Gather information	10/2-14/2	17/2-21/2	24/2-28/2	3/3-7/3	10/3-14/3	17/3-21/3	24/3-28/3	31/3-4/4	7/4-11/4	14/4-18/4	21/4-25/4	28/4-2/5	5/5-9/5	12/5-16/5	19/5-23/5
Define requirements															
Generate design alternatives															
Finalise design concept															
Mechanical & electrical design															
Bill of materials															
Intermediate presentation															
Order parts															
Assembly															
Programming															
Integration															
Write manual															
Testing															
Report															
Final presentation															

Table 23: Gantt chart